(4) Results of Chemical Analysis

Results of chemical analysis for drill core samples are presented in Figures 9, 10 and 11 together with the core logging results.

Although pyritized and silicified rocks are widely distributed in the Mt. Upao target area, no drill core sample from holes MJPP–1 and MJPP–2 reaches ore grades in any element. In hole MJPP–3, Ag contents generally range from 0.2 to 0.6 g/t to the depth of approximately 96 meters from the surface, with the maximum Ag content of 1.0 g/t for the interval between 3.0 and 3.5 meters. Copper contents of the same hole range between 0.005 and 0.047 % in the section deeper than 116 meters.

A gold content of 0.2 g/t was detected in a sample of porous silicified and hematitized andesite in the interval between 161.2 and 162.62 meters in hole MJPP–3. Some samples of pyritized andesite in the same hole indicated up to 0.47 % Cu where chalcopyrite was identified by hand lens. However, no elements are concentrated to a degree of commercial grade in hole MJPP–3.

Aiming at interpreting correlation and behavior of chemically analysed elements, principal component analysis was made for elements such as Au, As, Fe, Cu, Hg, Mo, Sb, Se and Zn. Ag, Pb and Mn, though chemically analysed, were excluded because the majority of the samples indicated values lower than detection limits for these three elements. Parameters of the principal component analysis are presented in Table 11.

The first principal component accounts for 26 % of the total variance, and has positive contribution from Au and As, and negative contribution from Cu, Mo and Zn. This component is related to Au concentration accompanied by Se and As. The results of the principal component analysis for the trench samples indicate associated concentrations of Au and Zn. Actually, average values of Au and Zn in the trench samples are about three fold higher than those in the drill core samples. This implies that Au had been primarily concentrated together with Se and As and later weathering and leaching resulted in relatively higher concentration of Au and Zn near surface.

The second principal component has positive contribution from Mn, Zn and Fe, and negative contribution from Hg, which may suggest Mn, Zn and Fe concentration in oxidized zones.

Contributions to the third principal component are largely from Cu, Hg and Fe, and may indicate a weak concentration of Cu in the Mt. Upao target area .

2–2–5 Assessment of Results

The Sibala formation, comprising mainly andesite lavas, is distributed in the Mt. Upao target area. The altered andesite member of the formation, being intensely hematitized and limonitized, occupies the tops of hills and ridges. This member had been formerlly distinguished as the Odiongan volcanics but was, in the course of the present Project including drilling campaigns, found to be transitional to an intensely pyritized, argillized and silicified part of the Sibala formation, which was later oxidized and leached near surface.

Intensely hematitized volcanic rocks, referred to here as the altered andesite member, appear to form mushroom shapes based on an interpretation of the drilling results as shown in Figure 12. The hematitized zones were formed presumably by oxidation, due to weathering, penetrating to depth through fractures and shear zones. The bottom of the hematitized zone which was drilled by three

holes, tends to become deeper southward from holes MJPP–1 through MJPP–2 to MJPP–3. In the hematitized altered volcanic rocks, quartz as a silica mineral and kaolinite as an acidic clay mineral are formed. Alunite was also observed in a number of samples.

The andesitic volcanics of the Sibala formation, underlying the altered andesite member, is entirely subjected to silicification or argillization associated with pyritization. Intense silicification and argillization are controlled by fracture systems and are partly developed with quartz veinlets or bands of extremely intense silicification. Alteration minerals are quartz as a silica mineral, sericite, sericite/montmorillonite interstratified minerals and montmorillonite which indicate neutral hydrothermal solutions. Alunite is occasionally formed in some samples.

As described above, there are distributed in the Mt. Upao target area alteration zones developed with quartz veinlets or silicified bands in parts of which traces of chalcopyrite are occasionally observed by hand lens. However, the results of the trenching and drilling failed to locate ore grade mineralization with any commercial significance, even though zones of anomalous concentrations of Au, or Cu are outlined in association with soil geochemical gold anomalies.

It is interpreted on the basis of the principal component analysis that Au had been primarily concentrated along with Se and As, and was later relatively enriched together with Pb due to weathering and leaching, because Au and Pb tend to remain in residual materials.

It is concluded that the above results do not support the continuation of further detailed exploration in the Mt. Upao target area.

2–3 Madarag

2–3–1 Geology, Alteration and Mineralization

(1) Geology

The geology of the Madarag target area is similar to that of the Mt. Upao target area which is located approximately three kilometers northeast as shown in the attached geological map. This area is distributed essentially with andesitic volcanic rocks of the Sibala formation and intruded by dacite dikes in its southern part. The volcanic rocks form the axial zone of a syncline trending in the NNW–SSE direction, judging from the structure of the underlying mudstone beds outcropping to the east and the west of the target area (MMAJ/JICA–MGB 1989).

The altered andesite member of the Sibala formation occupies the tops of hills in this area as is the case in the Mt. Upao target area, and intensely silicified bands are distributed in the E–W or NNE–SSW direction.

(2) Alteration

All the samples submitted to X–ray diffraction analysis were so intensely altered that no plagioclase was detected as shown in Table 5. Alteration mineral assemblages of quartz–sericite and quartz–sericite/montmorillonite interstratified minerals are identified in the volcanic rocks previously referred to as the Sibala formation. Those in the altered andesite member, the former Odiongan volcanics, are quartz–diaspore, quartz–diaspore–pyrophyllite and quartz–pyrophyllite, often accompanied by alunite, all of which commonly occur in high temperature acidic facies of hydrothermal activity.

(3) Mineralization

In this target area, there are no mineral occurrences which were mined or explored in the past, though geochemical anomalies in such elements as Au, As, Hg, Cu, Zn, Te and Se have been recognized (MMAJ/JICA–MGB 1989).

2–3–2 Geochemical Prospecting

(1) Methodology

Detailed soil geochemical sampling on grid basis (line spacing; 200 meters, sampling interval; 50 meters, number of samples; 200) was carried out for the Madarag target area and semi–detailed sampling on ridge–and–spur basis (number of samples; 104) for the periphery of the target area. Results of chemical analysis of soil samples for eleven elements, Au, Ag, As, Bi, Cu, Hg, Mo, Pb, Sb, Zn and Mn were statistically examined by using univariate and principal component analyses.

(2) Data Processing and Statistical Analyses

Statistical parameters are shown in Table 12 for the univariate analysis and in Table 13 for the principal component analysis.

Unlike in the Mt. Upao target area, 72 % of all the samples yielded Ag values exceeding its lower detection limit, while most values for Sb were lower than its detection limit. The average values for Au, Ag, Bi, Cu, Zn and Mo in the target area were about two fold higher and the average Pb value three fold higher than those in the Mt. Upao target area, while the average values for As and

Table 12 Statistic Parameters for Soil Samples, Madarag, 1991

Statistic Parameters

COMP. NAME	UNIT	NUM. DATA	MAXIMUM	MINIMUM	MEAN (M)	STD. DEV. (SD)	M-2×SD	M-SD	M+SD	M+2×SD
AU	ppb	164	76	1	9.7	0.363	1.8	4.2	22.4	51.6
AG	ppm	120	0.55	0.05	0.091	0.298	0.023	0.046	0.180	0.358
AS	ppm	167	80.2	0.2	5.34	0.463	0.63	1.84	15.50	44.99
BI	ppm	162	13.2	0.2	0.47	0.314	0.11	0.23	0.97	1.99
CU	ppm	167	353.0	3.0	35.15	0.381	6.08	14.62	84.48	203.09
HG	ppm	55	0.4	0.1	0.14	0.208	0.05	0.09	0.23	0.37
MO	ppm	166	52.8	0.2	2.83	0.574	0.20	0.76	10.62	39.84
PB	ppm	167	361.0	2.5	13.84	0.364	2.59	5.99	31.98	73.87
SB	ppm	45	0.8	0.2	0.30	0.200	0.12	0.19	0.47	0.75
ZN	ppm	167	272	1	8.8	0.596	0.6	2.2	34.8	137.4
MN	ppm	160	2960	10	73.1	0.677	3.2	15.4	347.1	1649.5

Correlation Matrix

	AU	AG	AS	BI	CU	HG	MO	PB	SB	ZN	MN
AU	---	120	164	159	164	55	163	164	45	164	157
AG	0.366	---	120	117	120	42	120	120	37	120	113
AS	0.431	0.044	---	162	167	55	166	167	45	167	160
BI	0.333	0.221	0.351	---	162	54	161	162	44	162	155
CU	-0.169	-0.039	-0.223	0.008	---	55	166	167	45	167	160
HG	0.223	-0.229	0.056	0.165	0.041	---	55	55	21	55	54
MO	0.477	-0.044	0.463	0.272	-0.171	0.203	---	166	45	166	159
PB	0.485	0.578	0.156	0.285	-0.070	0.184	0.137	---	45	167	160
SB	0.384	0.234	0.059	0.132	0.092	0.083	0.014	0.389	---	45	43
ZN	-0.239	0.112	-0.255	-0.090	0.614	-0.057	-0.501	0.040	0.120	---	160
MN	-0.265	0.075	-0.289	-0.047	0.567	-0.093	-0.565	-0.007	0.140	0.868	---

Table 13 Results of Principal Component Analysis for Soil Samples, Madarag, 1991

PRIN COMP	EIGEN VALUE	CONTRIB	CUM CONTRIB		AU	AG	AS	BI	CU	MO	PB	ZN	MN
P 1	3.248	0.361	0.361	EIGENVECTOR	-.363	-.095	-.342	-.215	.329	-.415	-.183	.431	.443
				FACTOR LOADING	-.654	-.172	-.616	-.388	.593	-.748	-.330	.777	.798
				CONTRIBUTION	.428	.029	.380	.150	.352	.559	.109	.604	.636
P 2	2.091	0.232	0.593	EIGENVECTOR	.337	.500	.109	.325	.231	-.032	.507	.334	.309
				FACTOR LOADING	.488	.723	.158	.470	.334	-.046	.733	.483	.447
				CONTRIBUTION	.238	.523	.025	.221	.112	.002	.537	.234	.200
P 3	1.142	0.127	0.720	EIGENVECTOR	.043	-.447	.419	.378	.461	.353	-.306	.162	.150
				FACTOR LOADING	.046	-.478	.448	.404	.492	.377	-.327	.173	.161
				CONTRIBUTION	.002	.228	.201	.163	.242	.142	.107	.030	.026
P 4	0.702	0.078	0.798	EIGENVECTOR	-.345	.037	.202	.660	-.424	-.440	-.135	-.049	.097
				FACTOR LOADING	-.289	.031	.169	.553	-.355	-.369	-.113	-.041	.081
				CONTRIBUTION	.083	.001	.029	.306	.126	.136	.013	.002	.007
P 5	0.626	0.070	0.868	EIGENVECTOR	.151	-.052	.699	-.492	-.315	-.206	-.037	.240	.205
				FACTOR LOADING	.119	-.041	.553	-.389	-.250	-.163	-.030	.190	.163
				CONTRIBUTION	.014	.002	.306	.152	.062	.027	.001	.036	.026
P 6	0.408	0.045	0.913	EIGENVECTOR	-.224	.720	.222	-.091	.258	.086	-.519	-.070	-.160
				FACTOR LOADING	-.143	.459	.142	-.058	.165	.055	-.332	-.045	-.102
				CONTRIBUTION	.020	.211	.020	.003	.027	.003	.110	.002	.010
P 7	0.387	0.043	0.956	EIGENVECTOR	.730	.028	-.268	.105	-.133	-.205	-.551	-.013	.140
				FACTOR LOADING	.454	.017	-.167	.065	-.083	-.127	-.343	-.008	.087
				CONTRIBUTION	.206	.000	.028	.004	.007	.016	.118	.000	.008
P 8	0.277	0.031	0.987	EIGENVECTOR	.161	-.125	.205	-.021	.508	-.640	.143	-.349	-.325
				FACTOR LOADING	.085	-.066	.108	-.011	.268	-.337	.075	-.184	-.171
				CONTRIBUTION	.007	.004	.012	.000	.072	.114	.006	.034	.029
P 9	0.120	0.013	1.000	EIGENVECTOR	.048	-.046	-.045	.087	-.064	-.085	-.046	.699	-.695
				FACTOR LOADING	.017	-.016	-.015	.030	-.022	-.030	-.016	.242	-.240
				CONTRIBUTION	.000	.000	.000	.001	.000	.001	.000	.058	.058

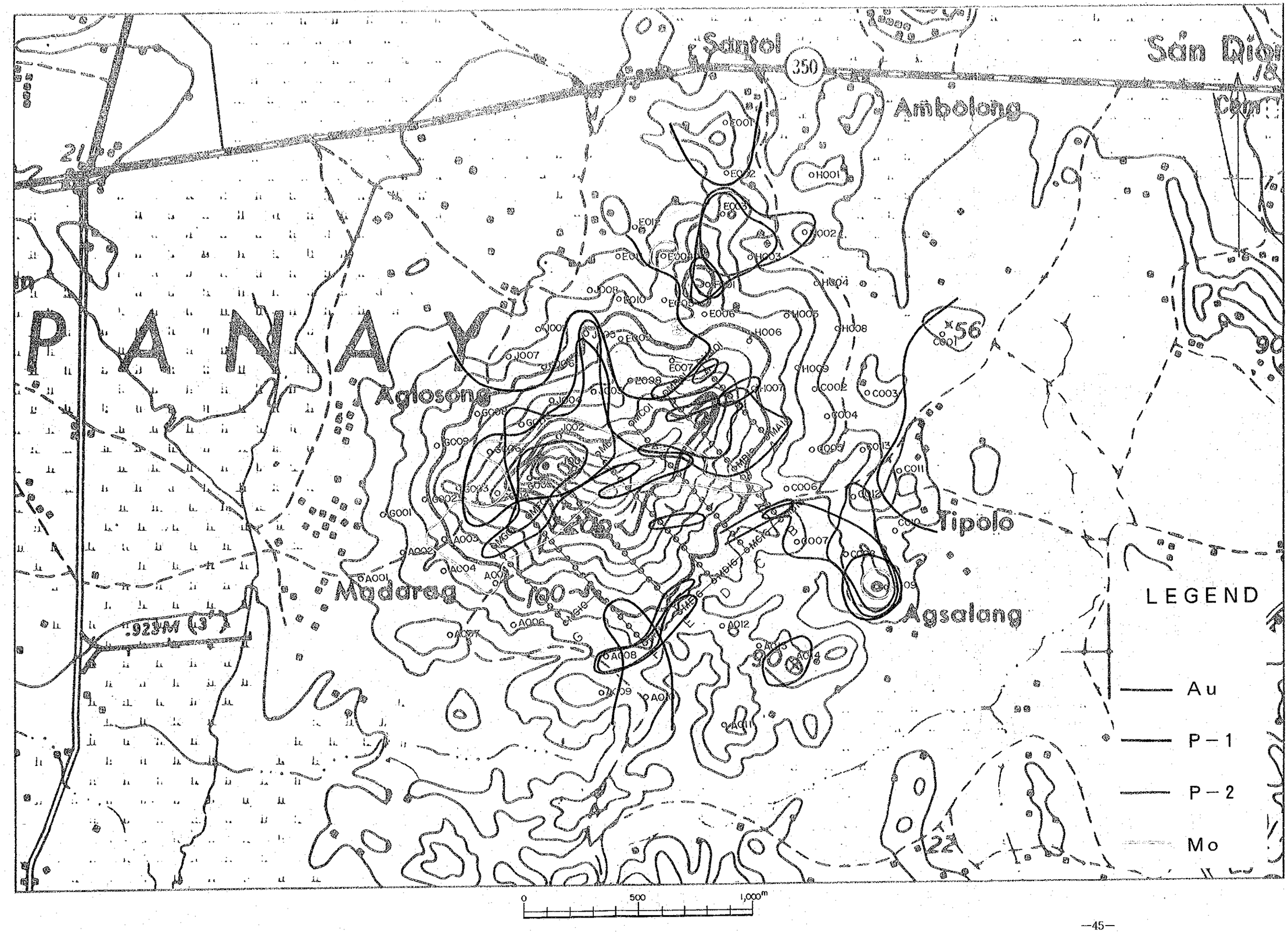

Figure 13 Geochemical Anomaly Map, Madarag, 1991

Sb were about 0.4 and 0.7 times respectively those in the Mt. Upao target area.

(3) Assessment of Geochemical Anomalies

The distribution of geochemical anomalies is shown in Figure 13.

According to the results of the univariate analysis, an intense geochemical gold anomaly including a maximum of 162 ppb is outlined by 52 ppb Au (M+2SD) and is elongated in the E–W direction. A less intense anomalous zone outlined by 22 ppb Au (M+SD) surrounds the intense gold anomaly and extends in the NNW–SSE direction. Ag and Mo values are higher than those in Mt. Upao target area. Mo values, in particular, include a maximum of 52.8 ppm but widely fluctuate with a high standard deviation.

According to the results of the principal component analysis, Mn and Zn in positive sense, and As, Mo and Au in negative sense, contribute considerably to the first principal component, as is the case in the Mt. Upao target area.

A negatively anomalous zone in the first principal component includes the Au anomaly of the univariate analysis, and extends further to the north and to the east. The anomalous zone may be related to concentrations of Mo, Au and As. Positive anomalies are considered to reflect only development and maturity of soils. Major elements which contribute to the second principal component are Pb, Ag, Au and Zn. This component appears to be related to concentrations of these elements. The Au anomaly of the univariate analysis overlaps a weakly anomalous zone of the component. Strongly anomalous zones are located on the southern extension of the survey line B and near Agsalang village.

2–3–3 Trenching

(1) Trenching Summary

Two trenches, with a width and depth of one meter, were excavated in the altered andesite member of the Sibala formation as shown in the attached geological map. A summary of the trenching particulars is tabulated below. MT–1 was excavated parallel to and MT–2 perpendicular to the drill hole MJPP–5.

Trenches

Trench No.	Bearing	Length(m)	No. of Samples
MT–1	210°	75	17
MT–2	300°	138	27

(2) Geology in Trench

The altered andesite member of the Sibala formation was exposed in each trench as shown in Figure 14. The rocks in the trench MT–1, being hematitized to variable degrees, are strongly argillized rather than silicified, although silicified fragments with obscure rims are often included. Hard silicified bands containing hematite were also observed in the trench. Thin silicification was often found with limited thickness of two to three milimeters near surfaces of exposed rocks in trench MT–2 and was coloured black due to development of hematite and goethite. Silicified bands with hematite were observed in the trench MT–2 as well.

Table 14 Analytical Results of Trench Samples, Madarag, 1992

Sample No.	Description of Sample	Analytical Results											
		Au	Ag	As	Sb	Cu	Pb	Zn	Mo	Fe %	Mn	Hg	Se
MT-1,004m	gry-pur weakly silicif fn grnd ad	22	0.2	36	0.8	16	60	5	63	4.50	<5	30	26.0
MT-1,010m	strong hm-Lm bg.wk arg soft ad	14	<0.2	10	0.2	46	48	6	10	6.20	<5	20	11.2
MT-1,015.0m	blue-gry brx(1cm)bg.milk wh alt ad	9	<0.2	12	0.6	34	143	4	26	5.00	<5	20	6.0
MT-1,018.7m	gry-pur colored weak arg soft ad	31	0.5	186	0.8	156	87	3	268	7.80	<5	10	34.0
MT-1,021m	ditto	9	<0.2	14	0.4	16	34	2	17	4.80	<5	10	10.0
MT-1,026m	gry-pur colored wkly silicif fn ad	18	0.4	26	0.4	13	98	3	43	5.10	<5	20	27.0
MT-1,030m	yel-brwn wkly silicif porous ad	12	<0.2	44	0.6	18	55	2	29	3.80	<5	10	1.8
MT-1,032m	hm-Lm/silicif black colored ad	50	0.4	64	0.4	86	197	5	55	19.80	<5	20	37.0
MT-1,038m	1-2mm hm v bg.wk arg alt andesite	47	<0.2	28	0.4	31	111	3	108	8.50	<5	20	32.0
MT-1,045m	bl-gry weakly silicif/hm v(1mm) bg.	54	0.4	58	0.2	24	91	3	48	8.30	<5	20	68.0
MT-1,050m	weakly arg soft andesite	26	0.3	14	0.2	92	112	3	133	5.00	10	20	34.0
MT-1,055m	ditto	37	<0.2	34	0.6	24	209	2	76	6.20	5	20	44.0
MT-1,059m	silicif-brx bg.gry-pur andesite	43	0.2	56	0.8	32	172	3	184	7.80	<5	60	53.0
MT-1,065m	lt gry brx bg.red-brwn andesite	333	0.5	374	6.4	79	104	3	138	6.60	<5	20	49.0
MT-1,066.5m	red-gry colored hard silicif ad	25	0.3	14	0.2	14	113	3	40	5.10	<5	20	38.0
MT-1,068.3m	dark gry v fine grained alt ad	97	<0.2	2	0.6	5	416	2	41	6.00	<5	10	<0.2
MT-1,073m	1-2mm hard surface bg.wk arg ad	36	<0.2	4	0.6	12	145		17	1.50	<5	20	<0.2
MT-2,002m	hm v(1mm) in crack,wk arg andesite	54	0.8	10	0.6	22	113	3	61	3.70	<5	20	20.0
MT-2,007m	ditto hm v bg.alt andesite	70	0.4	64	0.2	46	113	4	99	11.00	5	20	42.0
MT-2,013m	hd black surface(silicif) bg.arg ad	55	0.2	62	0.6	25	37	2	69	7.80	<5	20	41.0
MT-2,015m	silicif crack bg.alt andesite	21	<0.2	12	<0.2	62	31	3	116	7.50	<5	20	3.6
MT-2,020m	gry-pur colored arg alt andesite	17	<0.2	10	<0.2	13	165	2	18	4.60	<5	20	6.2
MT-2,025m	ditto, 1mm hm veinlets bg.	43	1.7	8	0.8	21	28	2	46	8.30	<5	20	11.0
MT-2,032m	ditto,1mm hm vein bg wk arg. ad	17	0.2	6	0.4	10	51	1	24	4.60	<5	20	5.8
MT-2,036m	ditto	22	0.5	4	0.4	19	95	2	42	5.80	<5	20	22.0
MT-2,040m	str silicif porous parts bg.	281	0.6	272	1.6	42	33	2	53	3.60	<5	10	18.0
MT-2,045m	ditto,with weaker silicif	551	0.4	84	0.8	86	10	3	38	3.80	<5	10	63.0
MT-2,050m	spotty hm bg.gry weakly arg ad	25	<0.2	8	<0.2	39	77	2	23	6.30	<5	20	12.0
MT-2,056m	milky wh wk arg alt andesite	30	<0.2	28	0.2	65	46	4	29	12.00	<5	20	18.0
MT-2,061m	gry wk arg andesite	323	0.3	150	1.2	47	8	1	41	3.30	<5	10	64.0
MT-2,065m	milky wh wk arg andesite	13	0.3	16	0.4	98	46	3	28	2.40	<5	10	32.0
MT-2,068.7m	hm vlt in ntwk bg. wk arg andesite	133	0.4	24	0.4	109	46	6	24	13.50	10	10	21.0
MT-2,075m	gry- pur colored wk arg andesite	24	<0.2	2	<0.2	44	42	1	6	2.90	<5	20	3.4
MT-2,078.5m	red-gry wk arg andesite	8	<0.2	2	0.2	10	68	2	5	2.00	<5	10	14.0
MT-2,084m	speccular hm bg. str arg ad	21	0.3	4	1.0	38	87	3	49	12.80	<5	20	38.0
MT-2,091m	ditto crystal bg.lt brwn ad	28	<0.2	2	0.2	12	52	1	50	1.60	<5	10	5.8
MT-2,095m	gry colored wk silicif/arg andesite	10	<0.2	2	<0.2	6	59	1	30	0.60	<5	10	5.6
MT-2,100m	bl-gry colored alt andesite	18	0.2	2	<0.2	22	43	2	21	7.80	<5	20	24.0
MT-2,105.5m	ditto	63	<0.2	4	0.2	24	104	2	80	6.50	<5	20	20.0
MT-2,111.7m	lt gry/milky wh alt andesite	9	0.9	32	<0.2	13	45	1	59	4.80	<5	20	5.4
MT-2,115.5m	red-gry v fn grained alt andesite	11	0.2	18	0.2	13	13	1	46	2.70	<5	30	31.0
MT-2,120m	bk hm grain(1-2mm)/vein bg.alt ad	10	<0.2	8	3.0	8	8	1	9	1.30	<5	30	1.6
MT-2,125m	1-2mm qtz pheno bg.wk silicif q-po?	512	0.5	2	1.0	10	10	1	15	1.20	<5	20	13.0
MT-2,130m	ditto	238	<0.2	36	0.6	30	30	2	15	3.80	<5	20	16.0

Au, Hg in ppb; Fe in %; other elements in ppm

Madarag MT-1 Trench

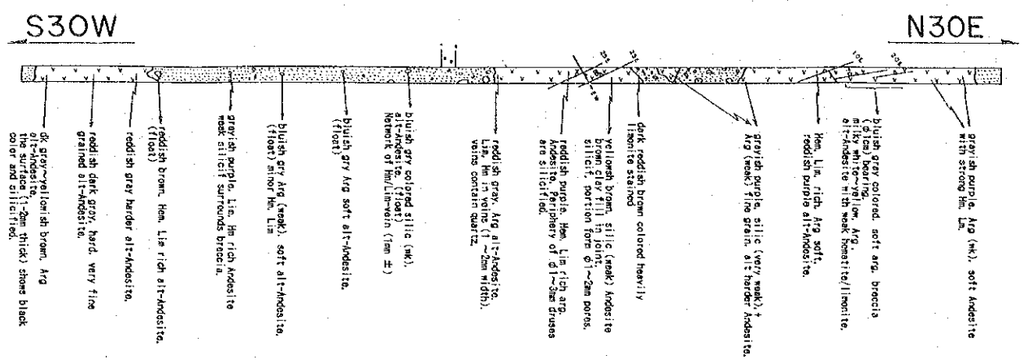

Madarag MT-2 Trench

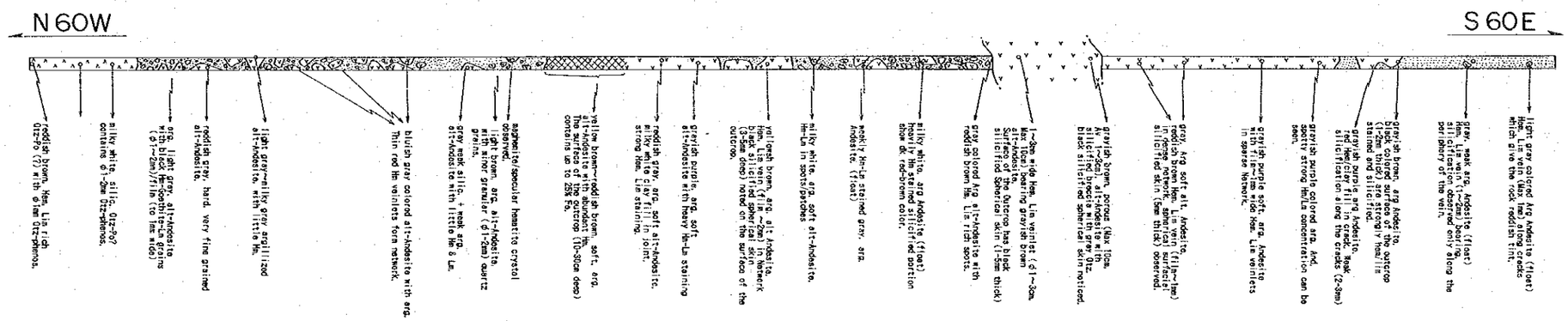

Figure 14 Geologic Map of Trenches, Madarag, 1992

0 10 20m

(3) Alteration in Trench

The results of X-ray diffraction analysis for 10 samples collected from the trenches are listed in Table 8, as well as those for drill core samples in other target areas.

All the samples were so intensely altered that no plagioclase was identified in any sample. Quartz was the major silica mineral detected in abaundance in all the samples. Hematite was also detected in appreciable amounts. Such high temperature-acidic minerals as diaspore and pyrophyllite were contained in many samples as well as kaolinite and alunite or natro-alunite. Pyrite remained in some sample.

(4) Results of Chemical Analysis

The results of Chemical analysis are presented in Table 14. A high concentration of Au, up to 333 ppb, was indicated in a sample collected in the trench MT-1 to the south of the hill top, and was associated with As, Pb and Mo values of 374, 104 and 138 ppm respectively. Two samples of silicified fragments with obscured rims in the trench MT-2 contained 551 ppb (maximum) and 281 ppb Au respectively. Other high values in Au were 323 ppb for a sample collected in the middle of the trench, and 212 and 288 ppb for quartz porphyritic samples at the west end. These high gold concentrations correspond closely to the soil geochemical anomalies and their values are rather high in comparison with those of the soil geochemical anomalies. Averages of individual elements of this target area are 14.8 times in Mo, 5.4 times in Pb, 3.1 times in Au, 2.8 times in Se and 1.7 times in As higher than those for the Mt. Upao target area. No meaningful differences were found for values of Cu, Fe and Zn in the two target areas, while the average value of Sb in this area is lower than that of the Mt. Upao target area.

Aiming at verifying behaviors of individual elements and mineralization-alteration characteristics, principal component analysis was made for results of chemical analysis of 44 samples collected in the two trenches. Parameters and results of the analysis are presented in Table 15.

The first principal component accounts for 35.2 % of the total variance. Major elements which contribute to the component are As, Se, Cu, Fe, Zn and Mo as well as Au to a less significant degree. The component is considered to indicate secondary enrichment of these elements in pyritic hydrothermal alteration zones due to weathering and leaching. The second principal component accounts for 19 % of the total variance. The component to which Sb, Au and Pb contribute in negative sense may suggest Au mineralization associated with Sb. The third principal component to which mostly Hg contributes may be ineffective for characterization of the mineralization, because the dynamic range of Hg is very narrow.

2-3-4 Drilling

(1) Drilling Summary

Two holes were drilled at the location shown in the attached geological map to the depth of approximately 300 meters with an inclination of -40°. These holes were aimed at exploring mineralization beneath a surface geochemical gold anomaly. A summary of drilling is tabulated below.

Drilling Summary

Hole No.	Depth(m)	Bearing	Inclination	Type of Rig	No. of samples
MJPP-4	300.00	165°	-40°	Long year 38	26
MJPP-5	300.91	210°	-40°	Long year 38	87

Table 15 Results of Principal Component Analysis for Trench Samples, Madarag, 1992

Statistic Parameters

COMP. NAME	UNIT	NUM. DATA	MAXIMUM	MINIMUM	MEAN (M)	STD. DEV. (SD)	M-2*SD	M-SD	M+SD	M+2*SD
Au	ppb	44	551	8	35.5	0.475 *	4.0	11.8	106.0	316.7
Ag	ppm	25	1.7	0.2	0.38	0.227 *	0.13	0.22	0.64	1.08
As	ppm	44	374	2	15.8	0.607 *	1.0	3.9	63.8	258.3
Fe	%	44	19.00	0.60	5.832	3.602	-1.371	2.230	9.433	13.035
Cu	ppm	44	156	5	26.5	0.356 *	5.1	11.7	60.2	136.7
Mn	ppm	5	10	5	7.6	0.147 *	3.8	5.4	10.6	14.9
Hg	ppb	44	60	10	17.4	0.169 *	8.0	11.8	25.7	38.0
Mo	ppm	44	260	5	38.5	0.369 *	7.0	16.5	89.8	210.1
Pb	ppm	44	416	8	64.1	0.342 *	13.3	28.2	140.8	309.3
Sb	ppm	37	6.40	0.20	0.509	0.342 *	0.105	0.231	1.118	2.457
Se	ppm	42	68.00	1.60	17.505	0.421 *	2.516	6.636	46.178	121.818
Zn	ppm	44	6	1	2.2	0.221 *	0.8	1.4	3.7	6.2

Correlation Matrix

	Au	As	Fe	Cu	Hg	Mo	Pb	Sb	Se	Zn
Au	---	44	44	44	44	44	44	37	42	44
As	0.455	---	44	44	44	44	44	37	42	44
Fe	0.137	0.284	---	44	44	44	44	37	42	44
Cu	0.347	0.559	0.513	---	44	44	44	37	42	44
Hg	-0.154	-0.005	0.150	-0.099	---	44	44	37	42	44
Mo	0.250	0.539	0.354	0.370	0.172	---	44	37	42	44
Pb	-0.066	-0.136	0.282	-0.105	0.205	0.254	---	37	42	44
Sb	0.405	0.372	-0.143	0.065	0.048	0.105	-0.183	---	35	37
Se	0.541	0.523	0.357	0.437	0.052	0.502	0.161	-0.024	---	42
Zn	0.103	0.357	0.627	0.577	0.091	0.282	0.356	-0.181	0.409	---

Results of Principal Component Analysis

PRIN COMP	EIGEN VALUE	CONTRIB	CUM CONTRIB		Au	As	Fe	Cu	Hg	Mo	Pb	Sb	Se	Zn
P 1	3.518	0.352	0.352	EIGENVECTOR	.294	.405	.356	.408	.043	.366	.104	.075	.409	.370
				FACTOR LOADING	.552	.760	.668	.766	.081	.686	.196	.142	.766	.694
				CONTRIBUTION	.304	.577	.446	.586	.007	.470	.038	.020	.587	.481
P 2	1.903	0.190	0.542	EIGENVECTOR	.402	.286	-.317	.059	-.249	-.030	-.479	.499	.029	-.333
				FACTOR LOADING	.554	.394	-.437	.082	-.344	-.041	-.661	.688	.040	-.459
				CONTRIBUTION	.307	.155	.191	.007	.118	.002	.437	.473	.002	.211
P 3	1.202	0.120	0.662	EIGENVECTOR	.039	.064	-.130	-.352	.658	.331	.319	.400	.046	-.215
				FACTOR LOADING	.043	.071	-.142	-.386	.722	.363	.350	.439	.051	-.236
				CONTRIBUTION	.002	.005	.020	.149	.521	.132	.123	.193	.003	.056
P 4	0.886	0.089	0.751	EIGENVECTOR	.393	-.182	-.218	-.313	-.454	.103	.473	-.203	.402	-.148
				FACTOR LOADING	.370	-.171	-.206	-.295	-.427	.103	.445	-.191	.379	-.140
				CONTRIBUTION	.137	.029	.042	.087	.183	.011	.198	.037	.144	.020
P 5	0.703	0.070	0.821	EIGENVECTOR	-.252	.183	-.242	-.021	.141	.427	-.411	-.547	.317	-.283
				FACTOR LOADING	-.212	.137	-.203	-.018	.119	.358	-.344	-.459	.266	-.237
				CONTRIBUTION	.045	.019	.041	.000	.014	.128	.118	.210	.071	.056
P 6	0.630	0.063	0.884	EIGENVECTOR	-.428	.239	-.086	.033	-.479	.524	.251	.191	-.385	-.021
				FACTOR LOADING	-.340	.190	-.068	.026	-.380	.416	.199	.151	-.306	-.017
				CONTRIBUTION	.115	.036	.005	.001	.145	.173	.040	.023	.093	.000
P 7	0.433	0.043	0.928	EIGENVECTOR	.212	-.333	.677	-.015	-.068	.302	-.147	-.020	-.179	-.486
				FACTOR LOADING	.140	-.218	.445	-.010	-.045	.199	-.097	-.013	-.118	-.320
				CONTRIBUTION	.020	.048	.198	.000	.002	.039	.009	.000	.014	.102
P 8	0.310	0.031	0.959	EIGENVECTOR	.183	-.490	-.414	.661	.149	.230	.117	-.020	-.164	-.033
				FACTOR LOADING	.102	-.273	-.230	.368	.083	.128	.065	-.011	-.091	-.018
				CONTRIBUTION	.010	.074	.053	.135	.007	.016	.004	.000	.008	.000
P 9	0.221	0.022	0.981	EIGENVECTOR	.517	.211	-.106	-.263	.101	.183	-.091	-.368	-.577	.296
				FACTOR LOADING	.243	.099	-.050	-.124	.047	.086	-.043	-.173	-.271	.139
				CONTRIBUTION	.059	.010	.002	.015	.002	.007	.002	.030	.074	.019
P10	0.194	0.019	1.000	EIGENVECTOR	.061	.487	.041	.315	.101	-.331	.399	-.269	-.167	-.528
				FACTOR LOADING	.027	.214	.018	.139	.045	-.146	.175	-.118	-.074	-.232
				CONTRIBUTION	.001	.046	.000	.019	.002	.021	.031	.014	.005	.054

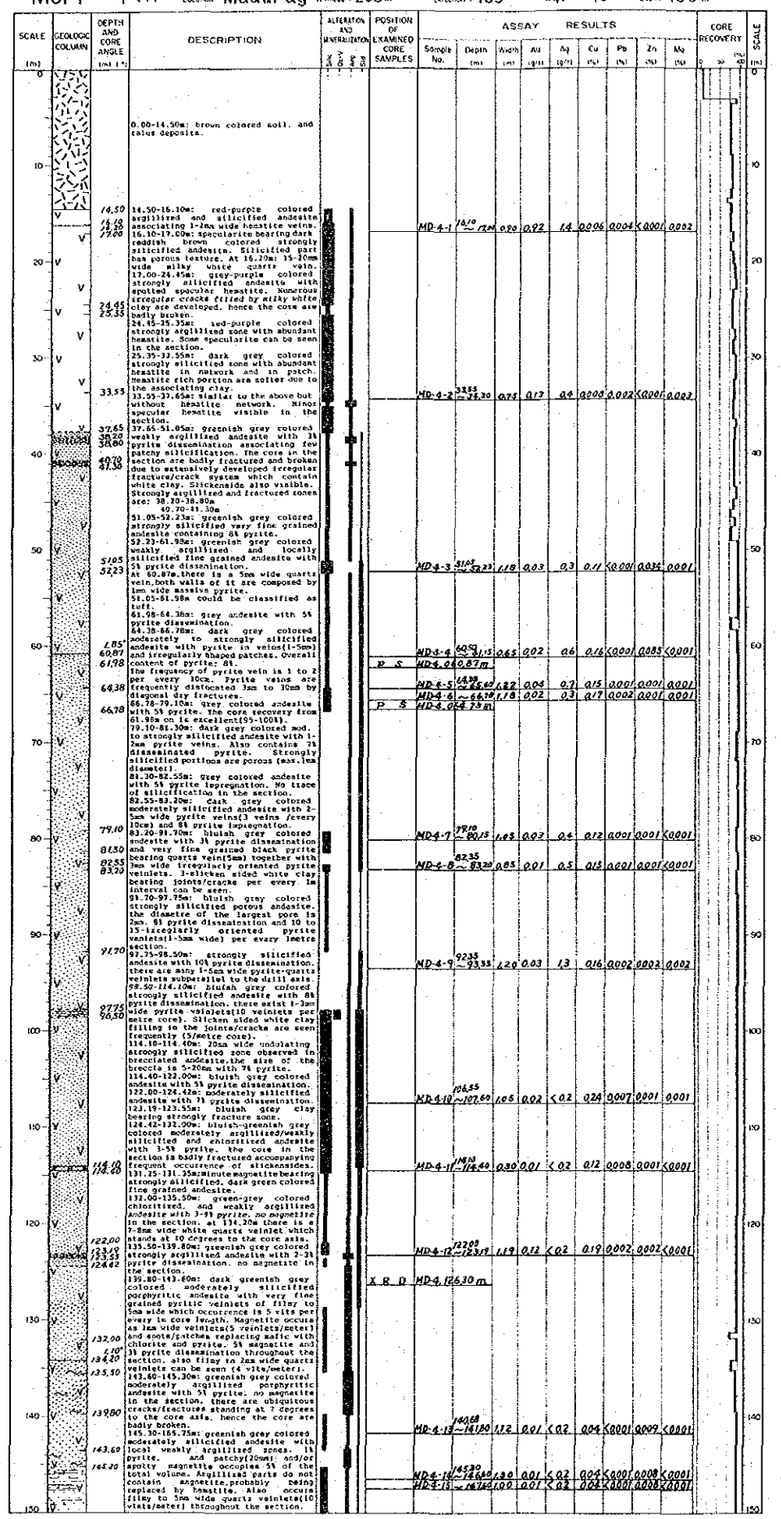

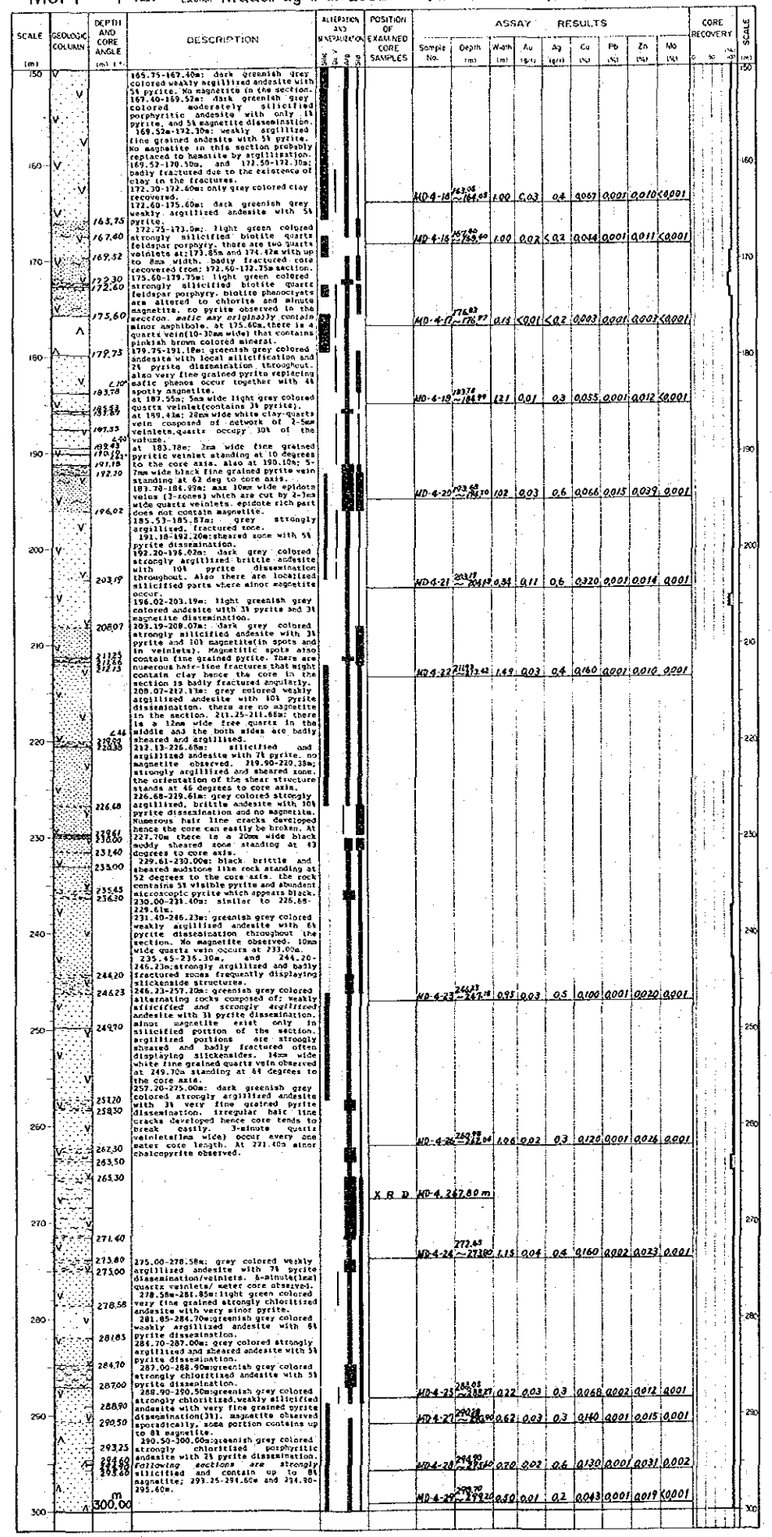

Figure 15 Geologic Log of MJPP–4, Madarag, 1992

MJPP－5 (1) Location Madarag Altitude 208m Direction 210° Angle －40° Depth 150m

SCALE (m)	GEOLOGIC COLUMN	DEPTH AND CORE ANGLE (m) (°)	DESCRIPTION	ALTERATION AND MINERALIZATION	POSITION OF EXAMINED CORE SAMPLES	ASSAY RESULTS									CORE RECOVERY	SCALE (m)
						Sample No.	Depth (m)	Width (m)	Au (g/t)	Ag (g/t)	Cu (%)	Pb (%)	Zn (%)	Mo (%)		
0			0–13.85m: tuffaceous deposit, hematite stained andesite boulder/pebble bearing brown colored soil/clay.													0
			13.85–15.00m: reddish purple colored weakly silicified andesite with 25% hematite in dissemination and in 0.5–2mm wide veinlets.													
10			15.00–21.25m: reddish purple colored moderately argillized and silicified andesite with 15% hematite in disseminated in veinlets, buff colored fine grained strongly silicified zone(vein) is seen at 18.35m to 18.65m(30cm wide) in which there are abundant irregular cracks filled with white clay (kaolinite?).													10
		13.85														
		15.00														
			21.25–23.10m: grey colored weakly silicified andesite with 2% disseminated pyrite, Hematite occur only in fissures at 22.40m(10mm wide) and 22.50m(5mm wide).													
20		18.25	23.10–25.07m: purplish grey colored moderately silicified porous, brecciated andesite with less than 1% pyrite and 5% hematite in dendritic cracks.													20
		21.25														
		23.10														
2.40		24.45														
2.45		25.07	25.07–32.85m: light grey colored strongly silicified fine grained andesite with very minor pyrite, hematite(3%) is seen only in dendritic cracks/fissures. 28.90–29.20m: porous andesite that has pyrite in the periphery of the pores which may amount to 2% of the total volume.													
		26.90														
		27.75														
30			32.85–37.45m: grey colored moderately silicified/auto-brecciated andesite with 3% pyrite dissemination. Irregular 0.5 to 2mm wide network of cracks filled with white clay are ubiquitous in the section.													30
		32.85														
		37.45	37.45–41.70m: purplish grey colored porous argillized andesite with 1% pyrite dissemination and specular hematite in wavy bands. Pores are also filled with specularite. Overall content of hematite is ca 20%.													
40		41.70	41.70–46.25m: grey colored strongly silicified andesite with 10% pyrite in dissemination and in less than 1mm wide veinlets. minor specks of chalcopyrite is seen at 42.35–46.20m section.													40
		46.25														
		47.00	46.25–47.00m: grey colored strongly argillized andesite with 5% very fine grained pyrite.													
50		51.00	47.00–53.90m: grey colored strongly silicified andesite with 8% pyrite in dissemination and 0.5mm to 8mm wide veinlets. At 51.80m and 52.90m there are quartz veins; the former being 7mm wide porous quartz vein standing at 25 degrees to the core axis, the former standing at 58 degrees to the core axis and has 10mm width with disseminated pyrite hence showing dark grey color. 10 to 15mm diameter anhydrite aggregates with blue and greenish tints are observed sporadically.													50
2.27		52.90														
2.88		53.90														
			53.90–58.75m: grey colored weakly argillized andesite with 5% pyrite dissemination. There are abundant irregular cracks accompanied by frequent slickensides hence the core tend to crumble easily.													
			58.75–59.20m: light grey colored strongly silicified andesite with 7% pyrite dissemination accompanying very minute and rare chalcopyrite.													
60		58.75	59.20–62.55m: dark grey colored weakly argillized andesite with 8% pyrite in dissemination and in veinlets.													60
		59.20														
		62.55	62.55–78.25m: light grey colored strongly silicified fine grained andesite with 8% pyrite dissemination, minor chalcopyrite at around 65.0m. Minor magnetite detected at 74.95 to 75.30m section.													
			78.25–86.65m: Similar strongly silicified andesite as above with 3–10% pyrite in dissemination and in patchy concentration. Sporadic chalcocite, bornite and possible cuprite specks are noted. At 79.00 base chalcopyrite speck in pyrite concentrated patch.													
70		78.25														70
		86.65	86.65–88.50m: grey colored strongly silicified, brecciated andesite with 2% overall pyrite in dissemination and in 5mm diameter patches.													
		88.50	88.50–92.60m: grey colored strongly silicified andesite with 5% pyrite dissemination throughout. at 91.85–92.60m, possible minute chalcocite(?) specs can be observed.													
80		92.60	92.60–95.00m: dark grey colored strongly argillized andesite with 5% pyrite dissemination. the breccia contained in the clay are all consisted of strongly silicified andesite.													80
		95.00	95.00–106.60m: grey colored strongly silicified andesite with 5–7% pyrite in dissemination and in 0.5–1mm wide veinlets. minute black possible chalcocite specs are observed in the section.													
			106.60–109.10m: grey colored weakly argillized andesite with 8% pyrite in dissemination and in 0.5–2mm wide veinlets. Joints/fractures standing at 80–90 degrees to the core axis predominate and they are filled with white clay(kaolinite).													
90		106.60														90
		109.10	109.10–113.30m: grey colored strongly silicified andesite with 5% pyrite dissemination very rare minute chalcocite specs are still visible in the section.													
		113.30	113.30–114.50m: dark grey colored weakly argillized andesite with 10% pyrite in dissemination and in 1–5mm wide veinlets. 3–5 sheared fractures filled with pyrite which stand at 10 degrees to the core axis observed in the section.													
		114.50	114.50–133.00m: grey colored strongly silicified andesite with 5 to 10% pyrite in dissemination and in 5–10mm wide veinlets. Minor chalcocite specks are visible throughout the section. Pyrite filling dendritic fractures can be seen at 116.6–131.0m.													
100			133.00–150.60m: grey colored strongly silicified andesite with 15–18% pyrite in dissemination and in less than 10cm wide veinlets. Minor chalcocite specks observed throughout the section. At 147.80–148.95m, two chalcopyrite specks observed. At 148.01 to 148.95m there is a coarse grained 20mm wide pyrite vein cutting much finer grained pyrite bearing quartz vein(black vein).													100
			150.60–155.80m: dark grey colored weakly argillized andesite with 15% pyritic dissemination very minor chalcopyrite specks recur sporadically.													
110																110
120																120
130																130
140																140
150																150

MJPP－5 (2) Location Madarag Altitude 208m Direction 210° Angle －40° Depth 300.91m

SCALE (m)	GEOLOGIC COLUMN	DEPTH AND CORE ANGLE (m) (°)	DESCRIPTION	ALTERATION AND MINERALIZATION	POSITION OF EXAMINED CORE SAMPLES	ASSAY RESULTS									CORE RECOVERY	SCALE (m)
						Sample No.	Depth (m)	Width (m)	Au (g/t)	Ag (g/t)	Cu (%)	Pb (%)	Zn (%)	Mo (%)		
150		150.60				MD-S-47	150.60–151.55	0.95	0.07	0.3	0.017	0.001	0.185	0.002		150
		155.80	155.80–158.50m: grey colored clay zone with 5% pyrite dissemination. No solid rock recovered from the section.			MD-S-48	153.40–154.40	1.40	0.05	<0.2	0.097	<0.001	0.022	0.006		
					XRD	MD-S-155.00m										
		157.80				MD-S-49	155.80–157.50	1.70	0.04	0.4	0.344	0.003	0.019	<0.001		
		158.50	158.50–160.55m: grey colored moderately argillized andesite with 3% pyrite dissemination.													
160		160.55	160.55–161.70m: dark grey colored moderately argillized andesite with 10% pyrite dissemination.													160
		161.70				MD-S-50	161.20–161.90	1.20	0.08	<0.2	0.035	<0.001	0.001	0.008		
		162.90	161.70–162.90m: dark grey colored moderately silicified andesite with 10% pyrite dissemination very rare minute chalcocite specks observed.			MD-S-51	162.80–163.80	0.90	0.18	0.3	0.105	<0.001	0.002	0.017		
			162.90–167.05m: dark grey colored weakly argillized andesite with 10% pyrite dissemination chalcopyrite speck observed at 163.50m.			MD-S-52	166.20–167.05	0.85	0.93	<0.2	0.074	<0.001	0.020	0.00		
		167.05			XRD	MD-S-168.90m										
170		170.05				MD-S-53	171.25–172.45	1.20	0.04	0.3	0.344	0.001	0.019	0.002		170
			167.05–170.05m: dark grey colored moderately argillized andesite with 8% pyrite dissemination.													
		176.45	170.05–176.45m: grey colored strongly argillized rock/site with 5% pyrite dissemination.			MD-S-54	176.45–177.30	0.85	0.02	1.5	0.192	<0.001	0.018	<0.001		
		177.30	176.45–177.30m: greyish grey colored moderately argillized chloritized feldspar porphyry with 3% pyrite dissemination.													
180			173.30–185.15m: grey colored strongly argillized andesite with 5% pyrite dissemination. 5 to 100mm sized strongly silicified rock fragments seen in the clayey matrix.													180
		185.15	185.15–185.40m: only sludge recovered, the grain consisted of quartz.													
		185.40														
			185.40–198.90m: grey colored strongly argillized andesite with 2% pyrite. At 189.60–193.10m, and 198.10–198.90m there occur ribbon very fine spotty chalcocite.			MD-S-55	189.60–191.60	2.00	0.05	0.9	0.378	0.004	0.027	0.001		
			198.90–202.00m: dark bluish green colored chloritized andesite with 3% pyrite in dissemination/veinlets and 15% magnetite in patchy concentration.			MD-S-56	189.10–191.50	1.50	0.04	0.4	0.326	0.002	0.011	<0.001		
190		189.60														190
		191.60														
		198.90				MD-S-57	199.10–199.90	0.80	0.04	0.5	0.193	0.004	0.012	<0.001		
		202.00	202.00–203.60m: light greenish grey colored chloritized, argillized andesite with 2% pyrite dissemination. No magnetite in the section.			MD-S-58	200.70–201.90	1.20	0.04	0.8	0.365	<0.001	<0.001	<0.001		
200		202.00				MD-S-59	201.90–203.10	1.20	0.05	0.8	0.394	<0.001	0.007	<0.001		200
		203.60	203.60–215.50m: dark bluish green colored chloritized, weakly argillized andesite with 3% pyrite in dissemination and in 0.5mm wide veinlets. Average magnetite content is 15% in patchy concentration and/or in veinlets. At 210.80m there is 6cm core length wide network white quartz veinlets zone.			MD-S-60	202.90–203.60	0.70	0.05	0.6	0.470	<0.001	0.007	<0.001		
						MD-S-61	204.80–205.85	1.20	0.05	0.9	0.427	<0.001	0.007	<0.001		
						MD-S-62	206.35–207.55	1.20	0.06	1.0	0.612	<0.001	0.008	<0.001		
					T.S	MD-S-205.22m										
210		210.80				MD-S-63	209.20–210.27	0.77	0.04	0.9	0.430	<0.001	0.008	<0.001		210
						MD-S-64	210.25–211.25	0.88	0.03	0.4	0.287	<0.001	0.011	<0.001		
		215.50	215.50–216.60m: grey colored argillized andesite with 3% pyrite in dissemination. No magnetite in the section.													
		216.60	216.60–237.80m: dark greenish grey colored weakly silicified andesite with 3% pyrite in dissemination and 15% magnetite in dissemination and in patchy concentration. rare and minute chalcopyrite specks occur in the section.			MD-S-65	216.40–217.30	0.88	<0.02	0.5	0.333	<0.001	0.020	<0.001		
		218.40														
		219.28				MD-S-66	219.28									
220					TS・FI	MD-S-219.23m										220
		227.40	227.40–237.70m: light greenish grey colored weakly argillized andesite with 5% pyrite in dissemination and in veinlets. No magnetite in the section. At 235.10–235.40m; very strongly argillized zone with 3% pyrite in dissemination.			MD-S-67	226.15–227.40	1.25	0.04	0.5	0.362	<0.001	0.013	<0.001		
						MD-S-68	227.40–228.60	1.20	0.04	0.5	0.477	<0.001	0.022	<0.001		
			237.70–238.70m: Strongly sheared, dark grey colored clayey zone containing 5–10mm diameter sub-angular breccia. 10% disseminated pyrite seen in the clay.													
		237.70	238.70–243.68m: light green colored strongly silicified hornblende feldspar porphyry with 3% pyrite dissemination.			MD-S-69	233.00–234.20	1.20	0.07	0.9	0.355	0.004	0.013	<0.001		
		238.70	Magnetite replacing hornblende phenos with chlorite pseudomorphs.		XRD	MD-S-238.00m										
			243.68–244.00m: strongly sheared zone similar to the above(237.7–238.7m) with 20% in dissemination.			MD-S-70	233.95–235.15	1.20	<0.02	<0.2	0.006	0.004	0.009	<0.001		
					TS・FI	MD-S-238.20m										
		243.68	244.00–266.45m: greenish grey colored chloritized, argillized andesite with 3 to 5% pyrite in dissemination and in veinlets. no magnetite in the section.													
		244.00	3 to 12mm wide white quartz veinlets are seen at; 246.72m, 248.85m, 248.05m, 249.10m, 252.10m, 253.2m, 258.80m, and 266.1m.													
		244.33														
		244.05														
		249.10				MD-S-71	249.05–250.30	1.15	0.04	<0.2	0.177	<0.001	0.004	<0.001		
250					XRD	MD-S-252.30m										250
		252.25	252.45–252.95m; strongly argillized, possibly sheared zone with 2% pyrite dissemination.													
		252.90	266.45–282.30m: greenish grey colored moderately silicified porphyritic andesite with 1% pyrite dissemination and 10% magnetite.			MD-S-72	255.00–255.78	0.78	<0.02	<0.2	0.034	<0.001	0.015	<0.001		
		6.10°	Minute specks of chalcopyrite seen rather abundantly at; 257.75–278.30m. minor amount of chalcopyrite can be observed throughout the section together with minor chalcocite(?) specks. up to 0.5mm wide quartz veinlet occurs in every 5cm core length. At 278.40m there is 8cm wide quartz vein containing pinkish red colored mineral.													
		256.10														
260		266.45														260
		6.20°	283.70–284.05m: dark greenish grey colored moderately silicified fine grained andesite with 1% pyrite in dissemination and 10% magnetite in dissemination, patchy concentration. very minor chalcocite(?) seen throughout the section. 0.5 to 3mm wide white quartz vein can be seen in every 5cm of core length.			MD-S-73	265.75–266.45	1.20	<0.02	0.3	0.048	0.002	0.013	<0.001		
		274.25				MD-S-74	266.25–267.35	1.10	<0.02	0.4	0.065	0.008	0.025	<0.001		
		6.52°	284.05–290.35m; greenish grey colored weakly silicified porphyritic andesite with 1% pyrite in dissemination, and 10% magnetite, very fine grained minor chalcopyrite(?) occurs in the section.													
		278.20				MD-S-75	274.05–275.25	1.20	0.02	0.2	0.051	<0.001	0.011	<0.001		
		279.05				MD-S-76	277.05–278.20	1.15	0.11	0.7	0.310	<0.001	0.012	<0.001		
280			290.35–294.85m: greenish grey colored chloritized, argillized andesite with 5% pyrite in dissemination no magnetite in the section. minute and minor chalcocite specks at 293.05m. quartz veins are seen at; 292.5m(3mm wide, contains long minute chalcopyrite), 292.75m(12mm wide), 293.0m(10mm wide), and 294.6m(7mm wide).			MD-S-77	278.05–279.05	1.00	0.03	<0.2	0.082	<0.001	0.011	<0.001		280
		280.30				MD-S-78	279.05–280.15	1.10	0.03	0.3	0.151	<0.001	0.015	<0.001		
		284.05				MD-S-79	280.15–281.40	1.25	0.03	0.2	0.095	<0.001	0.013	<0.001		
		285.30				MD-S-80	281.40–282.75	1.35	0.03	0.8	0.172	0.004	0.013	<0.001		
		6.45°														
		290.35														
		294.85	294.85–300.91m;End of the Hole; greenish grey colored moderately silicified porphyritic andesite with 5% pyrite and 5% magnetite in dissemination. rare and minute chalcocite and chalcopyrite specks seen in the section. quartz veins associating epidote concentration at the periphery of the veins are seen at; 297.2m(12mm wide), 297.28m(10mm wide), and 299.35m(10mm wide).													
300		300.91														300

Figure 16 Geologic Log of MJPP–5, Madarag, 1992

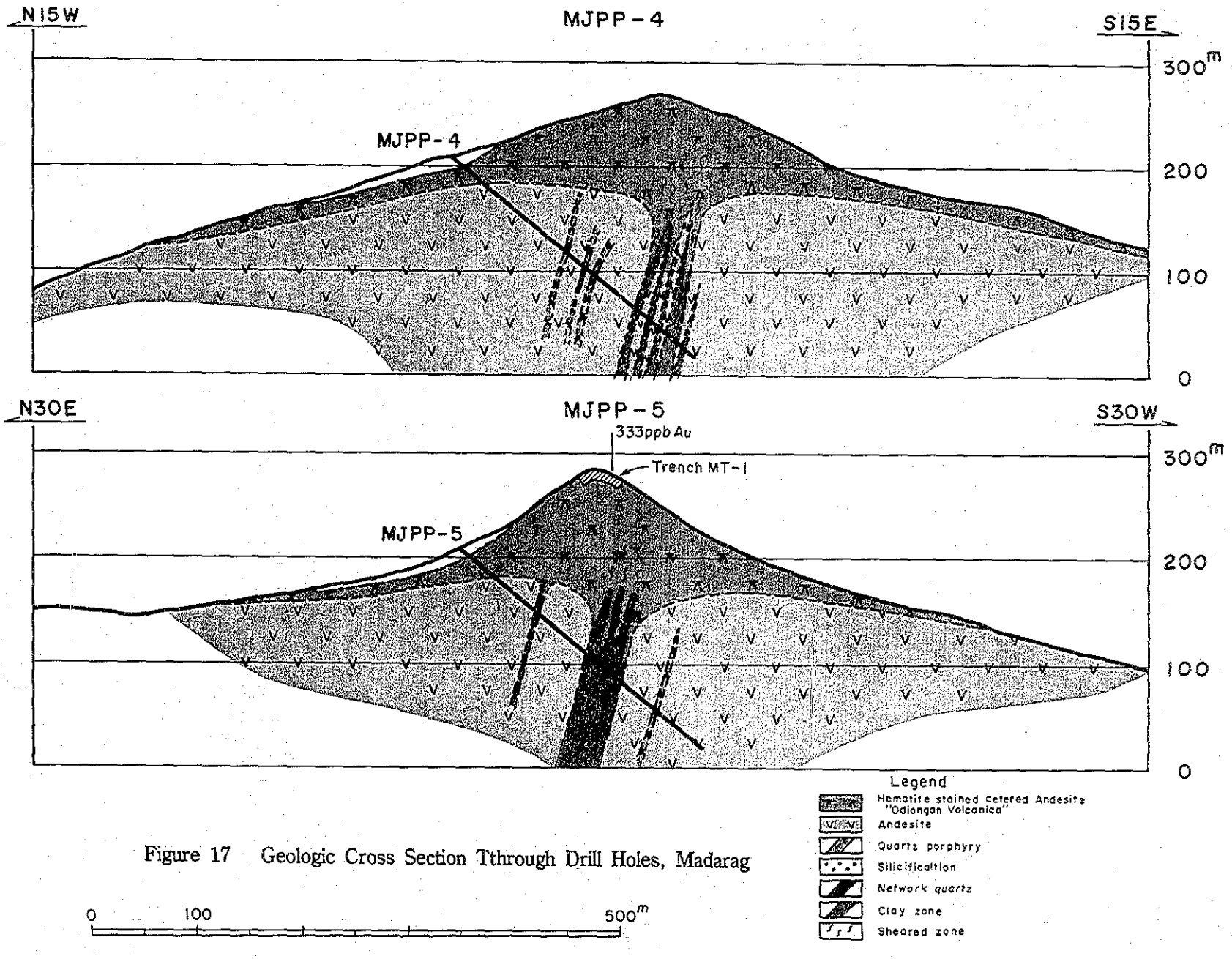

Figure 17 Geologic Cross Section Tthrough Drill Holes, Madarag

(2) Geology in Drill Holes

The two holes intersected soil–terrace deposits and the altered andesite and the pyroxene andesite members of the Sibala formation and porphyrite as shown in Figures 15 and 16. The apparent thicknesses of the soil–terrace deposits were 14.5 meters in MJPP–4 and 13.85 meters in MJPP–5. The soil–terrace deposits consist of andesitic fragments in unconsolidated soil matrices.

The altered andesite member was intersected between 14.5 and 37.65 meters in MJPP–4 and between 13.85 and 41.7 meters in MJPP–5. The bottom depths of the member appear to be shallower than those intersected in the drill holes of the Mt. Upao target area. The rocks of the altered andesite member, consist of reddish purple argillized andesite containing a large amount of hematite, commonly associated with silicification or quartz veinlets. Specularite, in association with hematite, occurs in many parts of the holes. Pyrite relicts were observed in places in MJPP–5. The altered andesite member had been previously distinguished as the Odiongan volcanics as is the case in the Mt. Upao target area. However, no hiatus was observed between the altered andesite and the underlying pyroxene andesite members in drill holes, with the one type grading in to the other. Accordingly, the altered andesite rocks are regarded in this report as a member of the Sibala formation.

The pyroxene andesite member started at depths of 37.65 meters in MJPP–4 and 41.7 meters in MJPP–5, and continued to the bottom of the holes. A porphyry dike was also intersected in the interval between 238.7 and 243.68 meters. The rocks consist mainly of coarse to medium grained, porphyritic propyletized pyroxene andesite lavas associated with pyrite dissemination and chloritization. Quartz and pyrite veinlets are often formed due to hydrothermal alterations such as silicification, argillization and pyritization. Magnetite was also observed in places.

Relatively intense silicification was intersected in intervals between 129.8 and 208.0 meters in MJPP–4 and between 266.45 and 290.35 meters in MJPP–5. MJPP–5 intersected three quartz veinlets containing epidote with thicknesses of approximately 10 mm below 297 meters depth.

(3) Alteration

Ten drill core samples which were submitted to X–ray diffraction analysis were so intensely altered, like the surface samples, that no plagioclase was detected as shown in Table 8. An alteration mineral assemblage of quartz–sericite ±chlorite–pyrite was common and indicates neutral condition for the hydrothermal solution. The mineral assemblage was commonly observed in association with a propylitic alteration, which is a relatively high temperature alteration facies. Calcite was detected in one sample. Hematite and alunite were identified only in a small number of samples.

(4) Results of Chemical Analysis

Results of chemical analysis for drill cores are presented in Figures 15 and 16 together with core loggings.

Of a total 29 samples from MJPP–2 which were submitted to chemical analysis, 76 % indicated 0.02 g/t Au or higher and 72 %, 0.2 g/t Ag or higher. Relatively high values recorded were 0.92 g/t Au and 1.4 g/t Ag, and 0.13 g/t Au and 0.4 g/t Ag in the hematitic sections between 16.1 and 17.0 meters and between 33.35 and 34.30 meters respectively, though they are far too low for commercial

Table 16 Results of Principal Component Analysis for Core Samples, Madarag, 1992

Statistic Parameters

COMP. NAME	UNIT	NUM. DATA	MAXIMUM	MINIMUM	MEAN (M)	STD. DEV. (SD)		M-2*SD	M-SD	M+SD	M+2*SD
AU	ppb	114	919	7	35.3	0.311	*	8.4	17.3	72.3	147.9
AG	ppm	92	2.1	0.2	0.50	0.259	*	0.15	0.27	0.91	1.65
AS	ppm	112	2900	1	12.6	0.817	*	0.3	1.9	82.5	541.0
FE	%	116	8.10	0.60	3.761	0.991		1.778	2.770	4.753	5.744
CU	ppm	116	8300	28	997.0	0.460	*	119.6	345.3	2878.2	8309.4
MN	ppm	105	1800	5	91.1	0.929	*	1.3	10.7	773.1	6563.7
HG	ppb	116	600	10	23.7	0.354	*	4.6	10.5	53.5	120.9
MO	ppm	116	173	1	6.4	0.479	*	0.9	2.8	25.2	76.0
PB	ppm	104	150	1	11.1	0.428	*	1.5	4.2	29.8	79.8
SB	ppm	44	15.50	0.20	0.550	0.492	*	0.057	0.177	1.708	5.304
SE	ppm	109	56.00	0.40	2.297	0.422	*	0.329	0.869	6.067	16.028
ZN	ppm	115	1850	1	30.8	0.748	*	1.0	5.5	172.1	963.2

Correlation Matrix

	AU	AG	AS	FE	CU	MN	HG	MO	PB	SE	ZN
AU	---	92	110	114	114	103	114	114	102	109	113
AG	0.366	---	88	92	92	88	92	92	83	90	91
AS	0.136	0.163	---	112	112	101	112	112	100	105	111
FE	0.271	0.150	0.039	---	116	105	116	116	104	109	115
CU	0.129	0.197	-0.019	0.232	---	105	116	116	104	109	115
MN	-0.218	-0.209	-0.673	0.144	0.173	---	105	105	94	98	104
HG	0.021	0.033	0.494	-0.015	0.067	-0.534	---	116	104	109	115
MO	0.281	0.053	0.571	0.149	0.069	-0.533	0.380	---	104	109	115
PB	0.085	-0.142	0.186	0.037	-0.007	-0.223	0.213	-0.003	---	98	103
SE	0.405	0.375	0.603	-0.026	-0.083	-0.726	0.401	0.613	0.134	---	108
ZN	-0.178	-0.209	-0.402	0.166	0.298	0.765	-0.056	-0.296	-0.045	-0.548	---

Results of Principal Component Analysis

PRIN COMP	EIGEN VALUE	CONTRIB	CUM CONTRIB		AU	AG	AS	FE	CU	MN	HG	MO	PB	SE	ZN
P 1	3.848	0.350	0.350	EIGENVECTOR	-.203	-.181	-.493	-.002	.043	.464	-.267	-.360	-.125	-.448	.343
				FACTOR LOADING	-.398	-.355	-.791	-.004	.084	.910	-.563	-.707	-.248	-.878	.673
				CONTRIBUTION	.159	.126	.626	.000	.007	.829	.317	.500	.061	.771	.453
P 2	1.711	0.156	0.505	EIGENVECTOR	.428	.374	-.027	.534	.518	.186	-.017	.105	.066	.033	.268
				FACTOR LOADING	.560	.489	-.036	.698	.677	.244	-.023	.137	.086	.044	.350
				CONTRIBUTION	.313	.239	.001	.488	.458	.059	.001	.019	.007	.002	.123
P 3	1.273	0.116	0.621	EIGENVECTOR	-.358	-.401	.245	.069	.270	.016	.564	.218	.148	-.115	.415
				FACTOR LOADING	-.404	-.453	.277	.078	.305	.018	.636	.246	.167	-.130	.468
				CONTRIBUTION	.163	.205	.076	.006	.093	.000	.405	.061	.028	.017	.219
P 4	1.066	0.097	0.718	EIGENVECTOR	-.062	.305	-.041	-.158	-.024	-.054	.128	-.412	.825	-.065	.041
				FACTOR LOADING	-.064	.315	-.043	-.163	-.025	-.056	.132	-.426	.852	-.067	.043
				CONTRIBUTION	.004	.099	.002	.027	.001	.003	.017	.181	.726	.004	.002
P 5	0.834	0.076	0.794	EIGENVECTOR	-.187	.395	-.018	-.592	.558	-.040	.121	-.120	-.334	.071	.004
				FACTOR LOADING	-.171	.360	-.016	-.541	.509	-.037	.111	-.109	-.305	.065	.004
				CONTRIBUTION	.025	.130	.000	.292	.260	.001	.012	.012	.093	.004	.000
P 6	0.620	0.056	0.850	EIGENVECTOR	.657	-.327	-.267	-.438	-.021	.074	.113	.148	.115	.131	.266
				FACTOR LOADING	.517	-.257	-.210	-.392	-.017	.058	.089	.117	.094	.103	.209
				CONTRIBUTION	.267	.066	.044	.154	.000	.003	.008	.014	.009	.011	.044
P 7	0.559	0.051	0.901	EIGENVECTOR	-.060	-.379	.072	-.088	.526	-.087	-.525	.217	.330	-.111	-.334
				FACTOR LOADING	-.045	-.283	.054	-.066	.393	-.065	-.393	.162	.246	-.083	-.250
				CONTRIBUTION	.002	.080	.003	.004	.154	.004	.154	.026	.061	.007	.062
P 8	0.446	0.041	0.941	EIGENVECTOR	-.225	.268	.285	-.219	-.227	.333	-.402	.435	.150	.231	.397
				FACTOR LOADING	-.150	.179	.191	-.146	-.152	.223	-.269	.291	.100	.154	.265
				CONTRIBUTION	.023	.032	.036	.021	.023	.050	.072	.084	.010	.024	.070
P 9	0.345	0.031	0.973	EIGENVECTOR	.321	-.110	.780	-.100	-.004	.062	-.120	-.423	-.126	-.211	.099
				FACTOR LOADING	.189	-.064	.458	-.059	-.002	.037	-.070	-.248	-.074	-.124	.058
				CONTRIBUTION	.036	.004	.210	.003	.000	.001	.005	.062	.005	.015	.003
P10	0.223	0.020	0.993	EIGENVECTOR	-.138	-.289	-.018	.135	.129	.111	-.100	-.430	-.009	.804	.090
				FACTOR LOADING	-.065	-.136	-.009	.064	.061	.053	-.047	-.203	-.004	.380	.043
				CONTRIBUTION	.004	.019	.000	.004	.004	.003	.002	.041	.000	.144	.002
P11	0.076	0.007	1.000	EIGENVECTOR	.033	-.009	.090	-.050	.013	.778	.306	.070	.069	.039	-.528
				FACTOR LOADING	.009	-.002	.025	-.014	.003	.214	.084	.019	.019	.011	-.146
				CONTRIBUTION	.000	.000	.001	.000	.000	.046	.007	.000	.000	.000	.021

grades.

Au values ranging from 0.12 g/t to 0.4 g/t were also recorded in parts of pyritic zones. Cu values higher than 0.1 % were recorded for 59 % of the total number of samples submitted to chemical analysis, with the maximum Cu value of 0.32 %. The sample which indicated the maximum Cu value also contained 0.11 g/t Au.

For samples from MJPP-5, only 13 of the total 87 samples indicated Au values lower than 0.2 g/t, with the maximum Au value of 0.54 g/t. Ag values higher than 0.2 g/t were recorded in 74 samples. Cu values were higher than 0.1 % in 51 samples, one of which showed the highest copper value of 0.83 % as well as 2.1 g/t Ag.

These assay results, though values are far too low for commercial interest, indicate that the Madarag target area is mineralized with Cu as well as Au and Ag. Judging from the generally high As contents, Cu-minerals were presumed to be of the energite-luzonite series, however, microscopic observation revealed Cu-minerals of the digenite-polybasite series.

Principal component analysis was made on the basis of the analytical results. Parameters of the principal component analysis are presented in Table 16.

Average values for the analysed elements are higher in this area than those in the Mt. Upao target area except for Fe, Hg and Se. Above all, Cu is 13.8 times, Au 11 times, Mn 7.2 times, Mo 5.6 times and Pb 3.2 times higher than those of the Mt. Upao target area. Analytical results of the drill core samples also indicated that base and precious metal contents of this area were much higher than those of the Mt. Upao target area as shown in the analytical results of the trench rock samples.

The first principal component accounts for 35 % of the total variance. Mn and Zn contribute in positive sense, and Se, As and Mo in negative sense to this component. Accordingly, the component is considered to be related to concentrations of Mn and Zn. The second principal component accounts for 16 % of the total variance. Major elements which contribute to this component are Fe, Cu, Au and Ag. The combination of these elements suggests that Cu mineralization which is observed in association with pyrite and magnetite in drill cores is accompanied by Au and Ag as well. The third principal component accounts for 16 % of the total variance and indicates Hg concentration. 27 % of the Au variance is accounted for by the sixth principal component to which Fe contributes in negative sense. This implies that there may be other types of Au concentration than that indicated by the second principal component, possibly Au enrichment near surface.

2-3-5 Assessment of Results

The Sibala formation, comprising mainly andesite lavas, is distributed in the Madarag target area. The altered andesite member of the formation, being intensely hematitized and limonitized, occupies the tops of hills and ridges. The altered andesite member was formed presumably by oxidation, due to weathering, penetrating to depth through fractures and shear zones. Such high temperature – acidic alteration minerals as diaspore and pyrophyillite are formed in the hematitic altered andesites. Kaolinite and alunite were also commonly observed. The pyroxene andesite member of the Sibala formation, underlying the altered andesite member, is entirely subjected to silicification or argillization associated with pyritization. Intense silicification and argillization are controlled by fracture systems and are partly developed with quartz veinlets or bands of extremely

intense silicification. The alteration of the andesitic volcanics comprises essentially neutral alteration mineral assemblages of quartz–sericite ± chlorite–pyrite with local development of hematite and alunite.

As described above, there are alteration zones developed with quartz veinlets or silicified bands in the Madarag target area. However, the results of the trenching and drilling failed to locate ore grade mineralization with any commercial significance, even though zones of anomalous concentrations of Au (maximum 0.92 g/t), or Cu (maximum 0.83 %) are locally associated with soil geochemical gold anomalies.

It is interpreted on the basis of the principal component analyses that unlike in Mt. Upao, Au in Madarag target area has been primarily concentrated along with Cu and Fe.

It is concluded that the above results do not support the continuation of further detailed exploration in the Madarag target area. However, it is important that Au and Cu in the target area are partially concentrated nearly to ore grades, which are the highest concentrations of the elements obtained to date in the Project Area. The Madarag target area may warrant additional work to examine a possibility of limited concentrations of Au and/or Cu for small scale mining operations, although there is very little chance to discover large scale ore deposits.

2–4 Nipa

2–4–1 Geology, Alteration and Mineralization

(1) Geology

The geology of the Nipa target area located approximately 9 kilometers south of the Madarag target area is essentially the same as that of Mt. Upao and Madarag with wide distributions of the andesitic volcanic rocks of the Silaba formation together with a quartz diorite intrusion along the coast to the north of Nipa village and also intruded quartz porphyry dikes to the south of the same village.

The quartz diorite intrusion had formerly been considered to be younger than the Sibala formation. The intrusion is, however, intruded by andesite dikes which are similar to a part of the Sibala formation in appearance. In addition, a K–Ar radiometric age of 30.1 ±1.5 Ma has been obtained for the quartz diorite (MMAJ/JICA–MGB, 1989) and, in turn, that of 25.7 ±1.9 Ma for the andesite dikes. Therefore, the possibility that the quartz diorite forms the basement of the Sibala formation in this area may not be discarded.

Volcanic rocks of the Sibala formation consist predominantly of lavas in the middle of the target area, and of pyroclostics in the eastern and western parts. Dark green, relatively fresh–looking basaltic lavas are distributed along the eastern and southern coast of the target area. Altered andesitic volcanic rocks characterized by hematitization are found on the tops of hills and ridges, as is the case in other target areas. The altered andesitic volcanic rocks are equivalent to the former Odiongan volcanics which are regarded as an altered andesite member of the Sibala formation in this report, as discussed in the previous sections for Mt. Upao and Madarag. Zones of intense silicification in the altered andesite member trend in the directions of NNE–SSW or E–W.

(2) Alteration

According to the results of the X–ray diffraction analysis as shown in Table 5, neutral alteration mineral assemblages such as quartz–chlorite ±montmorillonite and quartz–chlorite/montmorillonite interstratified minerals were identified, often together with albite, in samples of the former Sibala formation excluding the present altered andesite member. These alteration mineral assemblages are commonly found in propylitic alteration zones. In turn, assemblages of quartz–kaolinite–Fe oxides, often accompanied by alunite, are common in the altered andesite member characterized by hematitization. High temperature–acid alteration minerals such as dickite, pyrophyllite and diaspore were also identified, as in Mt. Upao target area, but are less abundant than in Madarag. Plagioclase, which is the most common rock forming mineral of volcanic rocks, was not detected in many samples due to extremely intense alteration.

(3) Mineralization

There are no mineral occurrences which have been mined in the past, however, base metal quartz veins carrying gold and silver, located to the south of Nipa village, were once explored by a Japanese company at the beginning of World War II. This ore deposit is described in the report by Abiog (1970). It is said that the ore deposit was explored by tunneling at 7 localities. Three old tunnels and about 200 tons of stock piles were found in the course of the present Project.

Locations of the tunnels and sketches in the tunnels are indicated in Figure 18.

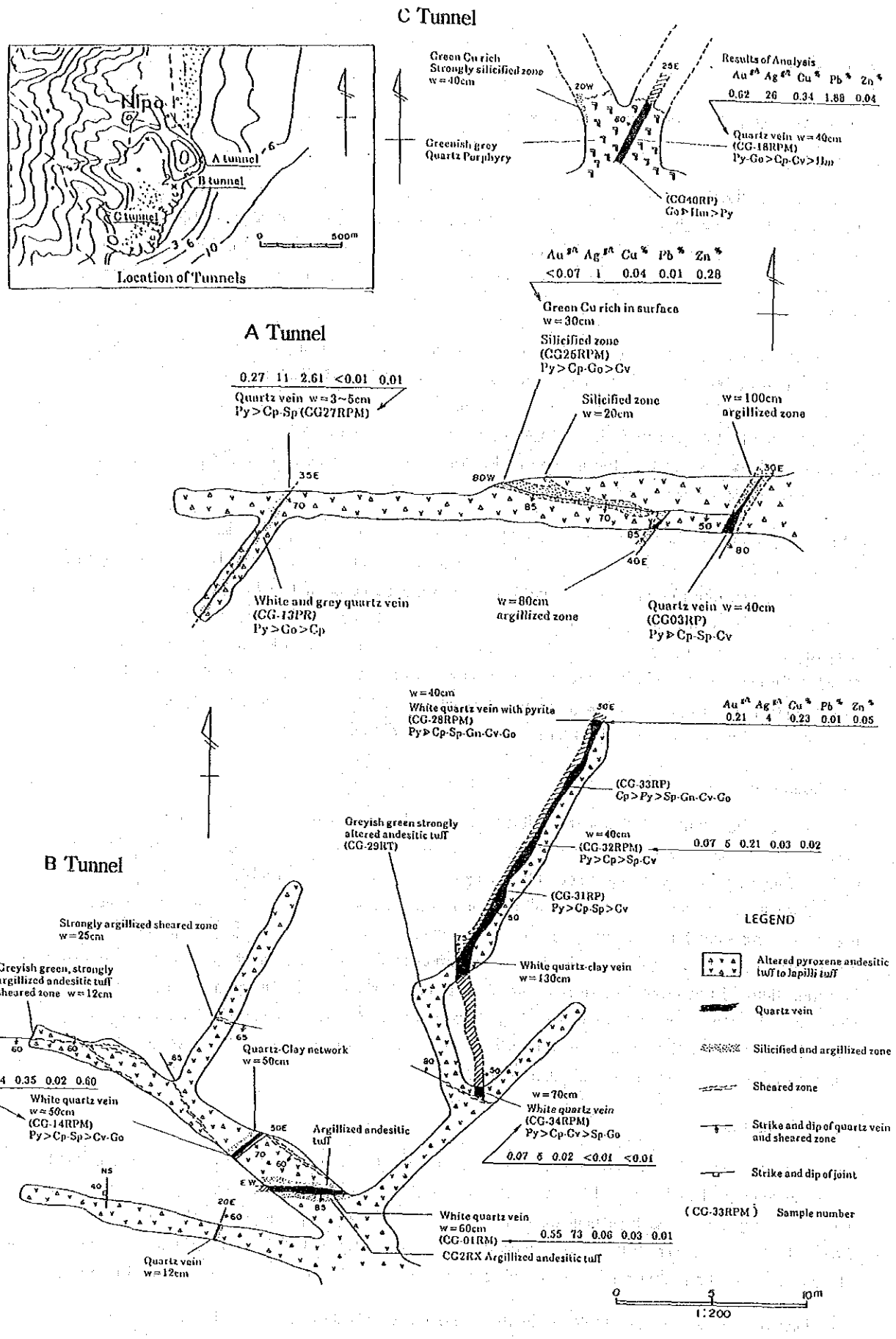

Figure 18 Vein Sketches of Nipa Deposit

The ore deposit, called Nipa, consists of quartz veins cross-cutting greenish grey, andesitic tuffs/lapilli tuffs of the Sibala formation and quartz porphyry intruding the Sibala formation. The veins were explored by cross-cuts in the NW-SE direction and drifts in the NE-SW direction. Major quartz veins strike in the directions ranging from N30° E to N50° E and dip 50° to 70° to the southeast. There are also discontinuous veins, striking in the E-W direction with steep dips and in the direction of N5° W with a dip of 50° to the east. Widths of veins range from a few tens of centimeters to 50 cm in general and widen up to approximately 130 cm in places. The quartz veins are slightly druzy and indicate comb or banded structures. Brown clay minerals are often formed within quartz veins or at the boundaries between quartz veins and host rocks. Ore minerals identified to date are pyrite, chalcopyrite, sphalerite, galena, covellite, chalcocite, goethite, hematite, magnetite, molybdenite, electrum and bournonite. Covellite and chalcocite are formed in cracks or rims of chalcopyrite. Galena occasionally includes molybdenite and rarely electrum. Maximum grades of samples collected in the tunnels are 0.62 g/t Au, 73 g/t Ag, 2.61 % Cu, 1.88 % Pb and 0.04 % Zn. A sample from the stock piles indicated 4.08 g/t Au and 115 g/t Ag.

Homogenized temperatures which were measured for 4 samples of quartz veins in the underground indicate, a unimodal distribution with a relatively sharp peak. Average homogenized temperatures ranged between 250℃ and 278℃ for three samples and was 233℃ for fourth sample (MMAJ/JICA-MGB,1992).

In addition to the Nipa ore deposit, gossanous zones are located in the vicinity of Puntales village in the northern part of the target area and are characterized by unique vegetation. Casual prospecting work in small scale was carried out for the gossanous zones in the past, however, no record has ever been published.

2-4-2 Geochemical Prospecting

(1) Methodology

Detailed soil geochemical sampling on a grid basis (line spacing; 200 meters, sampling interval; 50 meters, number of samples; 200) was carried out for a selected area adjacent to the west of the Nipa ore deposit and semi-detailed sampling on a ridge-and-spur basis (number of samples; 104) for the entire target area in the fiscal year 1991. The univariate and principal component analyses for the assay results of the soil samples led to outlining geochemical anomalies of Mo, Au, and other elements in the semi-detailed prospecting area adjacent to the detailed prospecting area. Two sub-target areas were selected for further detailed geochemical prospecting on a grid basis in the fiscal year 1992; one (Puntales) adjacent to the north of and the other (Apiton) adjacent to the west of the 1991 detailed prospecting area. The grid systems for the two sub-targets were the same as for the 1991 detailed prospecting area. Numbers of samples were 108 for Puntales and 202 for Apiton.

The samples were analysed for 12 elements, namely Au, Ag, As, Fe, Cu, Mn, Hg, Mo,Pb, Sb, Se and Zn. The assay results were interpreted by univariate and principal component analyses.

The results of the detailed geochemical prospecting are described below.

(2) Nipa

Parameters of the univariate analysis and those of the principal component analysis are presented in Tables 17 and 18 respectively. Distributions of geochemical anomalies are shown in Figure 19.

Table 17 Statistic Parameters for Soil Samples, Nipa, 1991

Statistic Parameters

COMP. NAME	UNIT	NUM. DATA	MAXIMUM	MINIMUM	MEAN (M)	STD. DEV. (SD)	M-2*SD	M-SD	M+SD	M+2*SD
AU	ppb	243	133	1	5.3	0.441	0.7	1.9	14.6	40.4
AG	ppm	167	0.40	0.05	0.072	0.230	0.025	0.042	0.122	0.208
AS	ppm	316	236.0	0.2	5.41	0.517	0.50	1.65	17.80	58.55
BI	ppm	242	3.8	0.2	0.40	0.316	0.09	0.18	0.83	1.72
CU	ppm	316	383.0	1.2	24.82	0.428	3.45	9.25	66.55	178.45
HG	ppm	98	0.3	0.1	0.13	0.174	0.06	0.08	0.20	0.30
MO	ppm	311	44.0	0.2	1.22	0.390	0.20	0.50	3.00	7.38
PB	ppm	315	113.5	0.5	6.15	0.407	0.94	2.41	15.71	40.14
SB	ppm	44	4.4	0.2	0.78	0.370	0.14	0.33	1.83	4.29
ZN	ppm	313	599	1	27.2	0.609	1.6	6.7	110.6	449.7
MN	ppm	314	2376	10	345.0	0.577	24.2	91.3	1303.4	4924.2

Correlation Matrix

	AU	AG	AS	BI	CU	HG	MO	PB	SB	ZN	MN
AU	---	148	243	198	243	76	242	243	40	241	243
AG	0.274	---	167	126	167	56	167	167	22	167	166
AS	0.595	0.165	---	242	316	98	311	315	44	313	314
BI	0.491	0.130	0.530	---	242	71	238	242	44	239	240
CU	-0.054	0.281	0.014	-0.047	---	98	311	315	44	313	314
HG	0.121	0.096	0.086	-0.127	-0.080	---	98	98	12	97	96
MO	0.372	0.187	0.198	0.052	0.183	-0.032	---	310	42	308	309
PB	0.414	0.388	0.486	0.290	0.349	0.040	0.140	---	44	312	313
SB	0.658	0.061	0.647	0.704	0.192	-0.150	0.214	0.773	---	43	43
ZN	-0.386	0.079	-0.321	-0.352	0.531	0.008	-0.347	0.160	-0.273	---	311
MN	-0.349	0.024	-0.324	-0.249	0.293	0.041	-0.469	0.090	-0.290	0.816	---

Table 18 Results of Principal Component Analysis for Soil Samples, Nipa, 1991

PRIN COMP	EIGEN VALUE	CONTRIB	CUM CONTRIB		AU	AG	AS	BI	CU	MO	PB	ZN	MN
P 1	3.152	0.350	0.350	EIGENVECTOR	.450	.145	.421	.366	-.093	.296	.215	-.404	-.399
				FACTOR LOADING	.800	.257	.748	.650	-.165	.526	.381	-.717	-.708
				CONTRIBUTION	.639	.066	.559	.422	.027	.277	.145	.515	.501
P 2	2.194	0.244	0.594	EIGENVECTOR	.145	.388	.180	.094	.501	.025	.502	.414	.334
				FACTOR LOADING	.215	.574	.267	.139	.743	.036	.744	.613	.494
				CONTRIBUTION	.046	.330	.071	.019	.552	.001	.554	.376	.244
P 3	1.184	0.132	0.726	EIGENVECTOR	-.073	.231	-.275	-.439	.332	.688	-.119	-.054	-.268
				FACTOR LOADING	-.080	.252	-.300	-.478	.361	.749	-.130	-.059	-.291
				CONTRIBUTION	.006	.063	.090	.228	.131	.560	.017	.003	.085
P 4	0.724	0.080	0.806	EIGENVECTOR	.044	.840	-.243	-.060	-.390	-.238	-.084	-.114	.026
				FACTOR LOADING	.037	.715	-.207	-.051	-.332	-.203	-.072	-.097	.022
				CONTRIBUTION	.001	.511	.043	.003	.110	.041	.005	.009	.000
P 5	0.556	0.062	0.868	EIGENVECTOR	-.263	.152	-.197	.700	.436	-.037	-.417	-.063	-.098
				FACTOR LOADING	-.196	.113	-.146	.522	.325	-.027	-.311	-.047	-.073
				CONTRIBUTION	.039	.013	.021	.272	.105	.001	.097	.002	.005
P 6	0.442	0.049	0.917	EIGENVECTOR	.659	-.129	-.356	.185	-.142	.287	-.282	.157	.426
				FACTOR LOADING	.438	-.086	-.237	.123	-.094	.191	-.187	.104	.283
				CONTRIBUTION	.192	.007	.056	.015	.009	.036	.035	.011	.080
P 7	0.347	0.039	0.955	EIGENVECTOR	-.230	-.138	-.585	.291	-.214	.171	.642	-.114	-.022
				FACTOR LOADING	-.135	-.081	-.345	.172	-.126	.101	.378	-.067	-.013
				CONTRIBUTION	.018	.007	.119	.029	.016	.010	.143	.005	.000
P 8	0.274	0.030	0.986	EIGENVECTOR	.461	-.105	-.384	-.178	.384	-.515	.108	-.094	-.406
				FACTOR LOADING	.241	-.055	-.201	-.093	.201	-.269	.056	-.049	-.212
				CONTRIBUTION	.058	.003	.040	.009	.040	.073	.003	.002	.045
P 9	0.127	0.014	1.000	EIGENVECTOR	.026	.014	-.008	.142	-.272	.056	-.046	.774	-.548
				FACTOR LOADING	.009	.005	-.003	.051	-.097	.020	-.017	.276	-.196
				CONTRIBUTION	.000	.000	.000	.003	.009	.000	.000	.076	.038

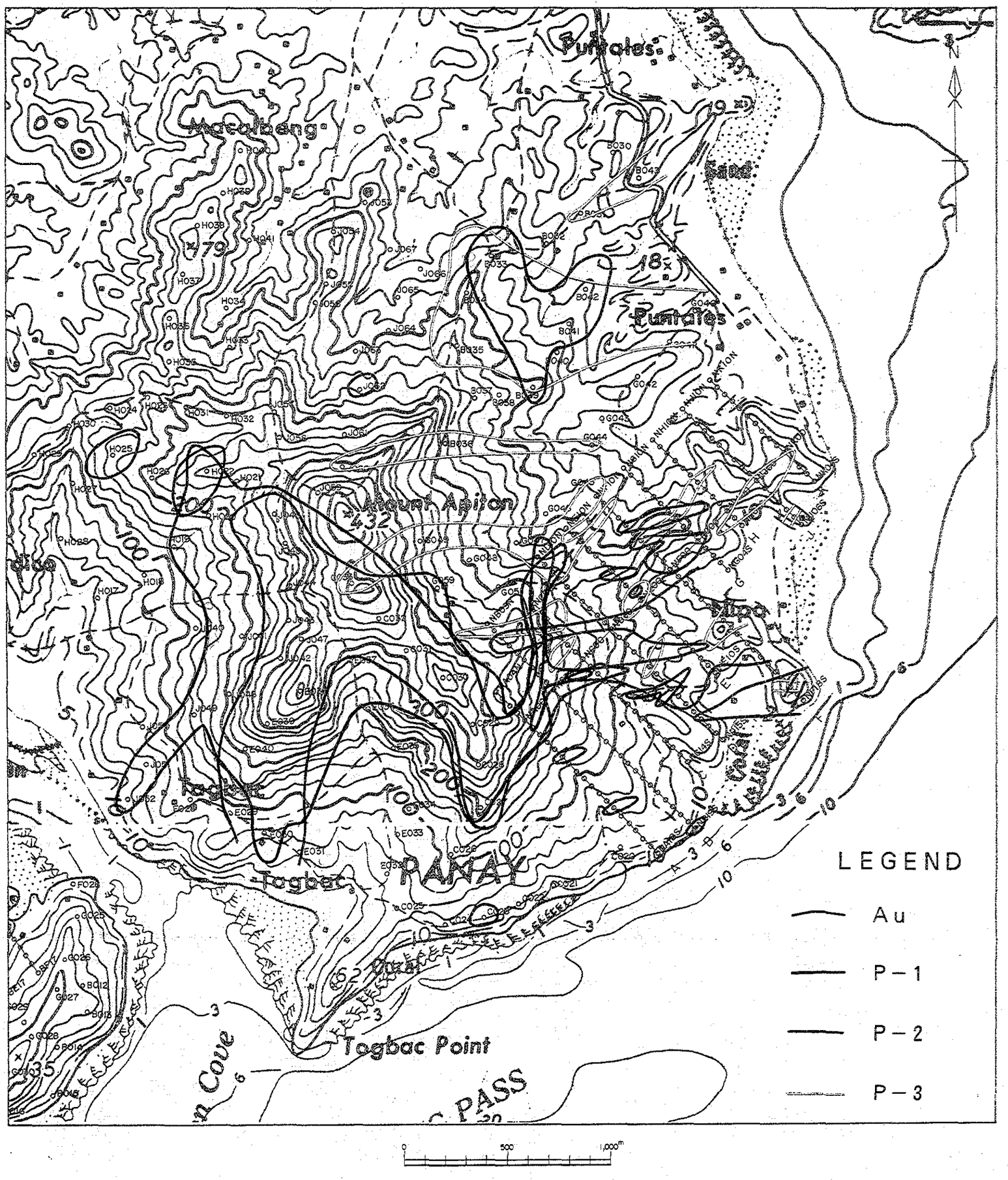

Figure 19 Geochemical Anomaly Map, Nipa, 1991

Au values exceeded the lower detection limit in 243 samples of the total 316, with an average of 5.3 ppb and maximum 133 ppb. High gold values (40 ppb or higher) were mostly located to the south of Mt. Apiton to the west of the 1991 detailed prospecting area, inside of which, no anomalous Au values were found. The average content of Cu was 25 ppm which was of a similar level to that in Mt. Upao. A maximum Cu value of 383 ppm was recorded. The average Zn value was 27 ppm, higher than that in Mt. Upao and in Madarag, and the highest Zn value reached 588 ppm. Pb values were similar to those of Zn.

The principal component analysis was made for 9 elements excluding Hg and Sb, most values of which were lower than the detection limit. The first principal component accounts for 35 % of the total variance, with Au, As, Bi and Mo contributing in a positive sense and Zn and Mn in a negative sense. The Au variance in the first principal component accounts for 64 % of the total variance of Au. This component, reflecting high correlation coefficients between Au, As and Bi, is considered to indicate Au concentrations. The distribution of anomalous positive scores in the component overlaps the gold anomalies outlined by the univariate analysis. The second principal component accounts for 24 % of the total variance, with positive contribution of Pb, Cu, Zn and Ag, and is considered to indicate concentration of base metal elements accompanied by Ag. The contribution of Au to this component is very small, which implies that the base metal concentration is not accompanied by Au mineralization. The cumulative contribution to the second principal component accounts for 59 % of the total variance. The third principal component accounts for 13 % of the total variance, with positive contribution of Ag, Cu and Mo and negative contribution of Au, As, Bi, Pb, Zn, and Mn. This component may indicate molybdenum mineralization accompanied by Cu, judging from Mo and Cu contributing in a positive sense to factor loading with negative contribution of Bi. The cumulative contribution up to the third principal component accounts for 72.6 % of the total variance.

(3) Puntales

Parameters of the univarite analysis and those of the principal component analysis are presented in Tables 19 and 20 respectively. Distributions of geochemical anomalies are shown in Figure 20.

The results of the 1991 work in the Nipa target area gave the average values of 5.3 ppb Au, 1.22 ppm Mo and 24.8 ppm Cu. In comparison with these averages, the results of the 1992 work indicated average lower in Au, at 3.7 ppb, and higher in Mo and Cu, at 2.9 and 38.6 ppm respectively. The hightest Au value was 99 ppb with only four samples ranging between 15 and 20ppb

The principal component analysis was made for 11 elements excluding Ag. The first principal component accounts for 36.3 % of the total variance with positive contributions of Mn, Zn and Hg and negative contributions of Mo, As and Au. Accordingly, it is expected that negatively anomalous scores in the first principal component outline molybdenum concentration accompanied by As and Au. The second principal component accounts for 22.7 % of the total variance with substantial contributions of Fe, Se, Cu and Au. Sb in a positive sense and Cu in a negative sense contribute substantially to the third principal component. Pb and As contribute to the fourth principal component in positive and negative senses respectively. However, positive or negative correlation between the elements contributing significantly to the third and fourth principal components may be doubtful in its effectiveness because Pb and Sb include many values less than the detection limits and have very narrow ranges of values. The cumulative contribution up to the fourth principal component accounts for 79 % of the total variance.

(4) Apiton

The parameters in the univariate analysis and the principal component analysis are presented in Tables 21 and 22 respectively. Distributions of geochemical anomalies are shown in Figure 20 together with those of the Puntales sub-target area.

The average Au value of 19.7 ppb is much higher than that of 5.3 ppb as obtained in the 1991 work in the Nipa target area. This average value is even higher than the threshold value of 14.6 ppb which outlines weak gold anomalies in the Nipa area. The average As value of 21.7 ppm is also higher than that of 5.4 ppm in the 1991 results. The average values of 0.7 ppm Sb and of 13.8 ppm Pb are a few times higher than those of 0.26 ppm Sb and 4.6 ppm Pb obtained in Puntales sub-target area, while the average value of 2.6 ppm Mo in this sub-target is comparable to that of 2.9 ppm Mo in the Puntales sub-target area.

The principal component analysis was made for 11 elements excluding Ag. Such elements as Sb, As, Se, Au, Pb, Fe and Mo contribute to the first principal component in a positive sense and Mn and Zn in a negative sense. High positive scores in this component may indicate Au concentration or mineralization. It is also observed in the Nipa target area that Au and As significantly contribute in a positive sense to the first principal component with negative contribution of Mn and Zn. Such elements as Mn, Zn, Hg, Cu and Mo significantly contribute to the second principal component with Mo in an opposite sense to the other elements. Mn and Zn are exceptional in contributing significantly to both the first and second principal components. It is difficult to coherently explain the second principal component. This component probably indicates concentrations of Zn and Mn, which are geochemically of little interest for the purpose of this project. Cu and Zn significantly contribute to the third principal component and Mo to the fourth principal component. However, values of these elements are generally low with maximum values of 158 ppm Cu, 106 ppm Zn and 33 ppm Mo which are regarded insignificant for exploration purposes.

The principal component analysis was made for the combined samples of the Puntale s and the Apiton sub-target areas and the parameters are presented in Tables 23 and 24 for the univariate and the principal component analyses.

The first principal component accounts for 39 % of the total variance with positive contributions of Au, As, Sb, Se and Pb and with negative contributions of Mn and Zn. This component apparently indicates Au mineralization accompanied by As, Sb and Se. It is expected that anomalous positive scores outline zones of gold mineralization. Mn, Zn and Hg contribute to the second principal component with a positive sense, and Mo with a negative sense. The meaning of the component is as interpreted in the case for the Apiton sub-target area. The third principal component, with significant contributions of Cu and Fe, may indicate Cu mineralization. However, Cu values are generally low both in Puntales and Apiton sub-target areas, which implies the sub-target areas are insignificant for copper exploration. The cumulative contribution up to the third principal component accounts for 75 % of the total variance.

2-4-3 Drilling

(1) Drilling Summary

A vertical hole (MJPP-6) was drilled to the depth of 300 meters as shown in attached geological map, aimed at exploring the geochemical anaomaly in the third principal component with significant

Table 19 Statistic Parameters for Soil Samples, Puntales, 1992

Statistic Parameters

COMP. NAME	UNIT	NUM. DATA	MAXIMUM	MINIMUM	MEAN (M)	STD. DEV. (SD)	M-2*SD	M-SD	M+SD	M+2*SD
AU	ppb	95	99	1	3.7	0.324 *	0.8	1.8	7.8	16.5
AG	ppm	4	0.2	0.2	0.20	0.000 *	0.20	0.20	0.20	0.20
AS	ppm	94	46	1	3.7	0.401 *	0.6	1.5	9.2	23.2
FE	%	108	9.10	0.30	3.274	1.714	-0.154	1.560	4.987	8.701
CU	ppm	108	232	1	38.6	0.355 *	7.5	17.0	87.4	198.1
MN	ppm	108	2200	20	136.4	0.653 *	5.4	25.0	586.9	2642.2
HG	ppb	108	80	10	37.3	0.184 *	16.0	24.5	57.0	87.0
MO	ppm	97	35	1	2.9	0.443 *	0.4	1.0	8.0	22.2
PB	ppm	91	70	1	4.5	0.358 *	0.9	2.0	10.5	24.1
SB	ppm	93	2.8	0.2	0.26	0.218 *	0.10	0.16	0.44	0.72
SE	ppm	93	6.2	0.2	0.74	0.332 *	0.16	0.35	1.59	3.43
ZN	ppm	108	180	1	14.5	0.609 *	0.8	3.8	59.9	239.5

Correlation Matrix

	AU	AS	FE	CU	MN	HG	MO	PB	SB	SE	ZN
AU	---	84	95	95	95	95	86	80	85	85	95
AS	0.497	---	94	94	94	94	85	80	83	81	94
FE	0.188	0.042	---	108	108	108	97	91	93	93	108
CU	0.201	-0.063	0.633	---	108	108	97	91	93	93	108
MN	-0.361	-0.326	0.448	0.373	---	108	97	91	93	93	108
HG	-0.141	-0.101	0.384	0.124	0.529	---	97	91	93	93	108
MO	0.458	0.338	-0.176	0.017	-0.656	-0.561	---	80	83	83	97
PB	-0.009	-0.169	0.183	0.226	0.229	0.386	-0.234	---	79	80	91
SB	0.319	0.477	0.041	-0.122	-0.264	0.063	0.167	0.095	---	85	93
SE	0.527	0.354	0.253	0.296	-0.463	0.063	0.456	0.122	0.347	---	93
ZN	-0.311	-0.310	0.538	0.420	0.900	0.530	-0.683	0.273	-0.206	-0.371	---

Table 20 Results of Principal Component Analysis for Soil Samples, Puntales 1992

PRIN COMP	EIGEN VALUE	CONTRIB	CUM CONTRIB		AU	AS	FE	CU	MN	HG	MO	PB	SB	SE	ZN
P 1	3.997	0.363	0.363	EIGENVECTOR	-.260	-.263	.215	.161	.457	.305	-.402	.172	-.183	-.238	.456
				FACTOR LOADING	-.519	-.526	.430	.323	.913	.610	-.804	.345	-.366	-.477	.911
				CONTRIBUTION	.269	.276	.185	.104	.834	.372	.646	.119	.134	.227	.830
P 2	2.452	0.223	0.586	EIGENVECTOR	.388	.261	.465	.419	.061	.224	.092	.223	.260	.440	.124
				FACTOR LOADING	.608	.409	.729	.657	.095	.351	.144	.348	.407	.688	.194
				CONTRIBUTION	.370	.167	.531	.432	.009	.123	.021	.122	.166	.475	.038
P 3	1.293	0.118	0.704	EIGENVECTOR	-.069	.256	-.200	-.490	-.035	.419	-.305	.270	.553	-.013	-.026
				FACTOR LOADING	-.078	.291	-.227	-.558	-.040	.477	-.347	.307	.629	-.015	-.030
				CONTRIBUTION	.006	.084	.052	.311	.002	.227	.121	.094	.395	.000	.001
P 4	0.985	0.090	0.793	EIGENVECTOR	-.101	-.501	-.190	.063	-.221	.084	.098	.694	-.159	.293	-.200
				FACTOR LOADING	-.100	-.497	-.189	.063	-.219	.083	.097	.689	-.158	.291	-.199
				CONTRIBUTION	.010	.247	.036	.004	.048	.007	.009	.475	.025	.085	.040
P 5	0.597	0.054	0.848	EIGENVECTOR	-.157	-.138	.139	-.169	-.165	.546	-.106	-.485	-.239	.470	-.160
				FACTOR LOADING	-.122	-.106	.107	-.131	-.127	.422	-.083	-.375	-.231	.363	-.124
				CONTRIBUTION	.015	.011	.011	.017	.016	.178	.007	.141	.053	.132	.015
P 6	0.510	0.046	0.894	EIGENVECTOR	.597	.300	-.188	-.183	.050	.195	-.122	.197	-.607	-.149	-.017
				FACTOR LOADING	.427	.214	-.134	-.131	.036	.139	-.087	.141	-.433	-.106	-.012
				CONTRIBUTION	.182	.046	.018	.017	.001	.019	.008	.020	.188	.011	.000
P 7	0.388	0.035	0.929	EIGENVECTOR	-.609	.651	-.112	.188	.040	.027	.151	.197	-.281	.117	-.036
				FACTOR LOADING	-.379	.406	-.070	.117	.025	.017	.094	.123	-.175	.073	-.023
				CONTRIBUTION	.144	.165	.005	.014	.001	.000	.009	.015	.031	.005	.001
P 8	0.283	0.026	0.955	EIGENVECTOR	-.120	.057	.748	-.482	-.217	-.215	.013	.227	-.159	-.128	-.061
				FACTOR LOADING	-.064	.031	.398	-.256	-.115	-.114	.007	.121	-.085	-.068	-.032
				CONTRIBUTION	.004	.001	.158	.066	.013	.013	.000	.015	.007	.005	.001
P 9	0.274	0.025	0.980	EIGENVECTOR	-.004	-.101	.037	-.158	.303	.392	.804	.007	.043	-.232	.028
				FACTOR LOADING	-.002	-.053	.019	-.104	.159	.205	.421	.004	.022	-.122	.015
				CONTRIBUTION	.000	.003	.000	.011	.025	.042	.177	.000	.000	.015	.000
P10	0.139	0.013	0.993	EIGENVECTOR	-.021	.012	.163	.421	-.266	.330	-.107	-.006	.062	-.553	-.543
				FACTOR LOADING	-.008	.004	.061	.157	-.099	.123	-.040	-.002	.023	-.206	-.203
				CONTRIBUTION	.000	.000	.004	.025	.010	.015	.002	.000	.001	.043	.041
P11	0.081	0.007	1.000	EIGENVECTOR	.012	-.021	.080	-.087	.705	-.168	-.140	.026	.019	.174	-.640
				FACTOR LOADING	.003	-.006	.023	-.025	.201	-.048	-.040	.008	.005	.050	-.182
				CONTRIBUTION	.000	.000	.001	.001	.040	.002	.002	.000	.000	.002	.033

Table 21 Statistic Parameters for Soil Samples, Apiton, 1992

Statistic Parameters

COMP. NAME	UNIT	NUM. DATA	MAXIMUM	MINIMUM	MEAN (M)	STD. DEV. (SD)	M-2*SD	M-SD	M+SD	M+2*SD
AU	ppb	202	165	1	19.4	0.405 x	3.0	7.6	49.4	125.6
AG	ppm	9	0.4	0.2	0.26	0.107 x	0.16	0.20	0.33	0.42
AS	ppm	202	384	2	21.7	0.447 x	2.8	7.7	60.7	170.0
FE	%	202	9.70	0.60	3.362	1.800	0.161	2.061	5.862	7.763
CU	ppm	202	158	2	22.4	0.314 x	5.3	10.9	46.0	94.9
MN	ppm	202	1200	5	63.0	0.495 x	6.4	20.2	197.3	517.2
MO	ppb	202	100	20	55.6	0.120 x	32.0	42.2	73.3	96.6
NO	ppm	199	33	1	2.6	0.319 x	0.6	1.3	5.5	11.4
PB	ppm	201	68	1	13.8	0.348 x	2.8	6.2	30.7	68.4
SB	ppm	173	15.0	0.2	0.70	0.438 x	0.09	0.25	1.90	5.21
SE	ppm	190	6.4	0.2	1.18	0.354 x	0.23	0.52	2.67	6.04
ZN	ppm	202	106	3	7.5	0.296 x	1.9	3.8	14.9	29.3

Correlation Matrix

	AU	AS	FE	CU	MN	MO	NO	PB	SB	SE	ZN
AU	---	202	202	202	202	202	199	201	173	190	202
AS	0.538	---	202	202	202	202	199	201	173	190	202
FE	0.318	0.473	---	202	202	202	199	201	173	190	202
CU	0.017	0.070	0.232	---	202	202	199	201	173	190	202
MN	-0.106	-0.235	-0.326	0.222	---	202	199	201	173	190	202
MO	0.459	0.243	0.023	-0.042	0.203	---	199	201	173	190	202
NO	0.232	0.150	0.247	0.036	-0.473	-0.108	---	198	171	188	199
PB	0.665	0.478	0.185	0.091	-0.052	0.344	0.177	---	172	189	201
SB	0.650	0.737	0.436	0.053	-0.202	0.242	0.189	0.524	---	164	173
SE	0.371	0.476	0.716	0.186	-0.550	0.002	0.457	0.345	0.417	---	190
ZN	-0.249	-0.248	-0.032	0.524	0.652	-0.077	-0.268	-0.289	-0.294	-0.367	---

Table 22 Results of Principal Component Analysis for Soil Samples, Apiton 1992

PRIN COMP	EIGEN VALUE	CONTRIB	CUM CONTRIB		AU	AS	FE	CU	MN	MO	NO	PB	SB	SE	ZN
P 1	4.032	0.367	0.367	EIGENVECTOR	.373	.386	.319	.025	-.256	.139	.233	.331	.390	.385	-.245
				FACTOR LOADING	.750	.776	.640	.050	-.514	.280	.467	.665	.782	.774	-.492
				CONTRIBUTION	.562	.602	.410	.002	.264	.078	.218	.443	.612	.599	.242
P 2	2.006	0.182	0.549	EIGENVECTOR	.260	.157	-.004	.301	.532	.383	-.298	.247	.197	-.184	.405
				FACTOR LOADING	.369	.222	-.005	.427	.754	.542	-.422	.350	.279	-.261	.574
				CONTRIBUTION	.136	.049	.000	.182	.568	.294	.178	.122	.078	.068	.330
P 3	1.673	0.152	0.701	EIGENVECTOR	-.188	-.007	.421	.581	-.006	-.345	.179	-.188	-.040	.281	.414
				FACTOR LOADING	-.243	-.009	.544	.764	-.008	-.446	.232	-.244	-.051	.363	.536
				CONTRIBUTION	.059	.000	.296	.584	.000	.199	.054	.060	.003	.132	.287
P 4	0.835	0.076	0.777	EIGENVECTOR	.203	-.372	-.325	.266	.053	.136	.673	.334	-.240	-.030	.009
				FACTOR LOADING	.185	-.340	-.297	.243	.049	.124	.615	.305	-.220	-.027	.008
				CONTRIBUTION	.034	.116	.088	.059	.002	.015	.378	.093	.048	.001	.000
P 5	0.666	0.061	0.837	EIGENVECTOR	-.033	-.241	.352	-.005	-.068	.720	-.089	-.249	-.375	.279	-.072
				FACTOR LOADING	-.027	-.197	.288	-.004	-.056	.587	-.072	-.203	-.306	.228	-.059
				CONTRIBUTION	.001	.039	.083	.000	.003	.345	.005	.041	.094	.052	.003
P 6	0.525	0.048	0.885	EIGENVECTOR	-.091	-.173	-.015	.258	-.029	-.211	-.516	.578	-.313	.258	-.292
				FACTOR LOADING	-.066	-.125	-.011	.187	-.021	-.153	-.374	.419	-.226	.187	-.211
				CONTRIBUTION	.004	.016	.000	.035	.000	.023	.140	.176	.051	.035	.045
P 7	0.394	0.036	0.921	EIGENVECTOR	-.424	.452	-.402	.481	-.274	.306	.006	-.093	.022	-.099	-.188
				FACTOR LOADING	-.266	.284	-.252	.302	-.172	.192	.003	-.058	.014	-.062	-.118
				CONTRIBUTION	.071	.080	.064	.091	.030	.037	.000	.003	.000	.004	.014
P 8	0.299	0.027	0.948	EIGENVECTOR	.478	-.393	-.196	.330	-.491	-.016	-.288	-.258	.259	-.195	-.019
				FACTOR LOADING	.261	-.215	-.058	.181	-.269	-.009	-.158	-.141	.142	-.107	-.005
				CONTRIBUTION	.068	.046	.003	.033	.072	.000	.025	.020	.020	.011	.000

Figure 20 Geochemical Anomaly Map, Puntales and Apiton, 1992

Table 23 Statistic Parameters for Soil Samples, Puntales and Apiton, 1992

Statistic Parameters

COMP. NAME	UNIT	NUM. DATA	MAXIMUM	MINIMUM	MEAN (X)	STD. DEV. (SD)	X-2*SD	X-SD	X+SD	X+2*SD
AU	ppb	297	165	1	11.5	0.507 *	1.1	3.6	36.8	118.4
AG	ppm	13	0.4	0.2	0.24	0.103 *	0.15	0.19	0.30	0.38
AS	ppm	296	384	1	12.3	0.563 *	0.9	3.4	45.0	164.5
FE	%	310	9.70	0.30	3.722	1.867	-0.011	1.855	5.589	7.455
CU	ppm	310	232	1	27.0	0.348 *	5.5	12.1	60.2	134.1
MN	ppm	310	2200	5	81.2	0.516 *	5.7	21.6	305.6	1148.9
MO	ppb	310	100	10	48.4	0.167 *	22.4	32.9	71.1	104.4
NO	ppm	296	35	1	2.7	0.365 *	0.5	1.2	5.3	14.5
PB	ppm	292	70	1	9.8	0.415 *	1.4	3.8	25.4	66.2
SB	ppm	266	15.0	0.2	0.50	0.428 *	0.07	0.19	1.32	3.52
SE	ppm	283	6.4	0.2	1.02	0.360 *	0.19	0.44	2.32	5.32
ZN	ppm	310	190	1	9.5	0.452 *	1.2	3.3	26.8	75.9

Correlation Matrix

	AU	AS	FE	CU	MN	MO	NO	PB	SB	SE	ZN
AU	---	286	297	297	297	297	285	281	258	275	297
AS	0.714	---	296	296	296	296	284	281	256	271	296
FE	0.291	0.388	---	310	310	310	296	292	266	283	310
CU	-0.190	-0.168	0.325	---	310	310	296	292	266	283	310
MN	-0.307	-0.341	-0.066	0.348	---	310	296	292	266	283	310
MO	0.459	0.411	0.233	-0.131	0.183	---	296	292	266	283	310
NO	0.159	0.100	0.071	0.064	-0.533	-0.320	---	278	254	271	296
PB	0.658	0.529	0.223	-0.084	-0.125	0.504	0.025	---	251	269	292
SB	0.687	0.738	0.392	-0.148	-0.296	0.361	0.096	0.559	---	249	266
SE	0.451	0.496	0.586	0.105	-0.543	0.154	0.409	0.364	0.468	---	283
ZN	-0.371	-0.361	0.164	0.501	0.787	0.101	-0.471	-0.218	-0.278	-0.390	---

Table 24 Results of Principal Component Analysis for Soil Samples, Puntales and Apiton, 1992

PRIN COMP	EIGEN VALUE	CONTRIB	CUM CONTRIB		AU	AS	FE	CU	MN	MO	NO	PB	SB	SE	ZN
P 1	4.250	0.380	0.380	EIGENVECTOR	.405	.405	.215	-.116	-.286	.197	.160	.331	.390	.355	-.281
				FACTOR LOADING	.838	.837	.445	-.239	-.592	.408	.331	.685	.807	.733	-.581
				CONTRIBUTION	.702	.700	.198	.057	.351	.167	.110	.469	.651	.535	.338
P 2	2.313	0.210	0.589	EIGENVECTOR	.125	.124	.264	.230	.460	.426	-.409	.225	.149	-.061	.459
				FACTOR LOADING	.190	.189	.401	.349	.699	.647	-.622	.342	.226	-.092	.698
				CONTRIBUTION	.036	.036	.161	.122	.489	.419	.386	.117	.051	.008	.487
P 3	1.644	0.149	0.738	EIGENVECTOR	-.124	-.057	.489	.596	-.042	-.260	.336	-.143	-.038	.386	.185
				FACTOR LOADING	-.159	-.074	.627	.764	-.054	-.333	.430	-.183	-.048	.494	.237
				CONTRIBUTION	.025	.005	.393	.584	.003	.111	.185	.033	.002	.244	.056
P 4	0.681	0.062	0.811	EIGENVECTOR	.246	-.121	-.449	.401	.207	-.035	.454	.521	-.053	-.193	-.011
				FACTOR LOADING	.203	-.100	-.371	.331	.171	-.029	.375	.430	-.044	-.160	-.009
				CONTRIBUTION	.041	.010	.137	.110	.029	.001	.140	.185	.002	.025	.000
P 5	0.543	0.049	0.860	EIGENVECTOR	-.134	-.378	.073	-.089	-.117	.570	.048	.227	-.537	.364	-.117
				FACTOR LOADING	-.098	-.279	.054	-.065	-.086	.420	.035	.167	-.396	.268	-.086
				CONTRIBUTION	.010	.078	.003	.004	.007	.176	.001	.028	.157	.072	.007
P 6	0.389	0.035	0.895	EIGENVECTOR	.178	.149	.046	-.167	.191	.436	.800	-.521	-.022	-.192	.143
				FACTOR LOADING	.111	.093	.029	-.104	.119	.272	.374	-.325	-.014	-.120	.089
				CONTRIBUTION	.012	.009	.001	.011	.014	.074	.140	.106	.000	.014	.008
P 7	0.330	0.030	0.925	EIGENVECTOR	-.018	-.425	.398	-.533	.145	-.246	.272	.336	.192	-.111	.242
				FACTOR LOADING	-.011	-.244	.229	-.306	.083	-.141	.156	.193	.110	-.064	.139
				CONTRIBUTION	.000	.060	.052	.094	.007	.020	.024	.037	.012	.004	.019
P 8	0.264	0.024	0.949	EIGENVECTOR	.653	.105	.265	-.064	.048	-.286	-.142	-.029	-.605	-.125	-.042
				FACTOR LOADING	.335	.054	.136	-.033	.025	-.147	-.073	-.015	-.311	-.064	-.022
				CONTRIBUTION	.113	.003	.019	.001	.001	.022	.005	.000	.097	.004	.000
P 9	0.230	0.021	0.970	EIGENVECTOR	-.513	.636	.156	-.124	.147	-.073	.174	.312	-.336	-.155	-.049
				FACTOR LOADING	-.246	.305	.075	-.060	.070	-.035	.084	.149	-.161	-.074	-.023
				CONTRIBUTION	.060	.093	.006	.004	.005	.001	.007	.022	.026	.006	.001
P10	0.182	0.017	0.987	EIGENVECTOR	.052	.107	-.323	-.250	.558	-.215	.013	-.056	-.036	.669	.061
				FACTOR LOADING	.022	.046	-.138	-.107	.239	-.092	.006	-.038	-.015	.286	.026
				CONTRIBUTION	.000	.002	.019	.011	.057	.008	.000	.001	.000	.082	.001
P11	0.144	0.013	1.000	EIGENVECTOR	-.059	-.174	.279	.125	.504	.040	-.041	-.080	.129	-.126	-.759
				FACTOR LOADING	-.022	-.066	.106	.047	.191	.015	-.016	-.030	.049	-.048	-.288
				CONTRIBUTION	.001	.004	.011	.002	.037	.000	.000	.001	.002	.002	.083

contributions of Cu and Mo. The anomaly was outlined around the gossanous zones which were located in the northern part of the Nipa target area by the 1991 work.

(2) Geology in Drill Holes

The results of core logging of MJPP–6 and the geological profile estimated from drilling are presented in Figures 21 and 22 respectively.

MJPP–6 from the collar to the bottom of hole, consists essentially of andesitic volcanics mostly comprising andesite lavas which belong to the Sibala formation. Tuffacious beds are intercalated within intervals between 17.6 and 22.2 meters and between 92.25 and 94.80 meters. The rocks are ubiquitously subjected to argillization, silicification and green alteration.

The rocks from the collar to 7.30 meters are intensely weathered, leached and argillized together with limonite and hematite dissemination. Those deeper than 7.30 meters are dark greenish grey, bluish grey or grey in colour and ubiquitously propylitized often with epidote. Pyrite dissemination is also ubiquitous. Intense argillization is developed within intervals between 22.2 and 41.8 meters, and 85.2 and 87.6 meters, the latter of which is highly fractured. An intensely fractured zone is intersected in the interval between 222.25 and 223.80 meters with an angle of 32° to the core axis. Fractured zones with intense silicification are developed within intervals between 122.35 and 123.5 meters, 126.5 and 131.8 meters and 188.2 and 194.1 meters. Other zones of intense silicification are intersected within intervals of 113 to 142 meters, 188.2 meters, 229.9 to 237.1 meters and 286.45 to 305.1 meters, often with druzy quartz veinlets. Anhydrite veinlets are also well developed. However, no concentrations of commercially useful metallic elements were observed.

(3) Alteration

The results of X–ray diffraction analysis of MJPP–6 drill core samples are presented in Table 8.

Alteration mineral assemblages of quartz–sericite ±chlorite ±albite were identified together with pyritization in most of the samples. No iron oxides were identified. The alteration mineral assemblages are common in propylitic alteration.

(4) Results of Chemical Analysis

As shown in Figure 21, assay results of 34 samples from MJPP–6 are commonly low in contents of commercially interesting metallic elements. Au values are less than 0.1 g/t. The maximum Ag value of 0.8 g/t is recorded for the intensely silicified samples with quartz veinlets within the interval between 59.2 and 59.3 meters. Cu values are also less than 0.02 %.

2–4–4 Assessment of Results

The Nipa ore deposit which was explored at the beginning of World War II, consists of pyrite–chalcopyrite quartz veins accompanied by small amounts of lead and zinc. The veins, with the maximum width of approximately 1.3 meters, are discontinuous with variable widths. The assay results of our samples indicated maximum values of 4.08 g/t Au, 115 g/t Ag and 2.61 % Cu. However, most of the samples were lower than 1 g/t Au, a few tens g/t Ag and 1 % Cu. The results of the geochemical soil sampling failed to prove a further extension of this mineralization. In addition, the ore deposit is located too close to the coast to be developed or explored extensively.

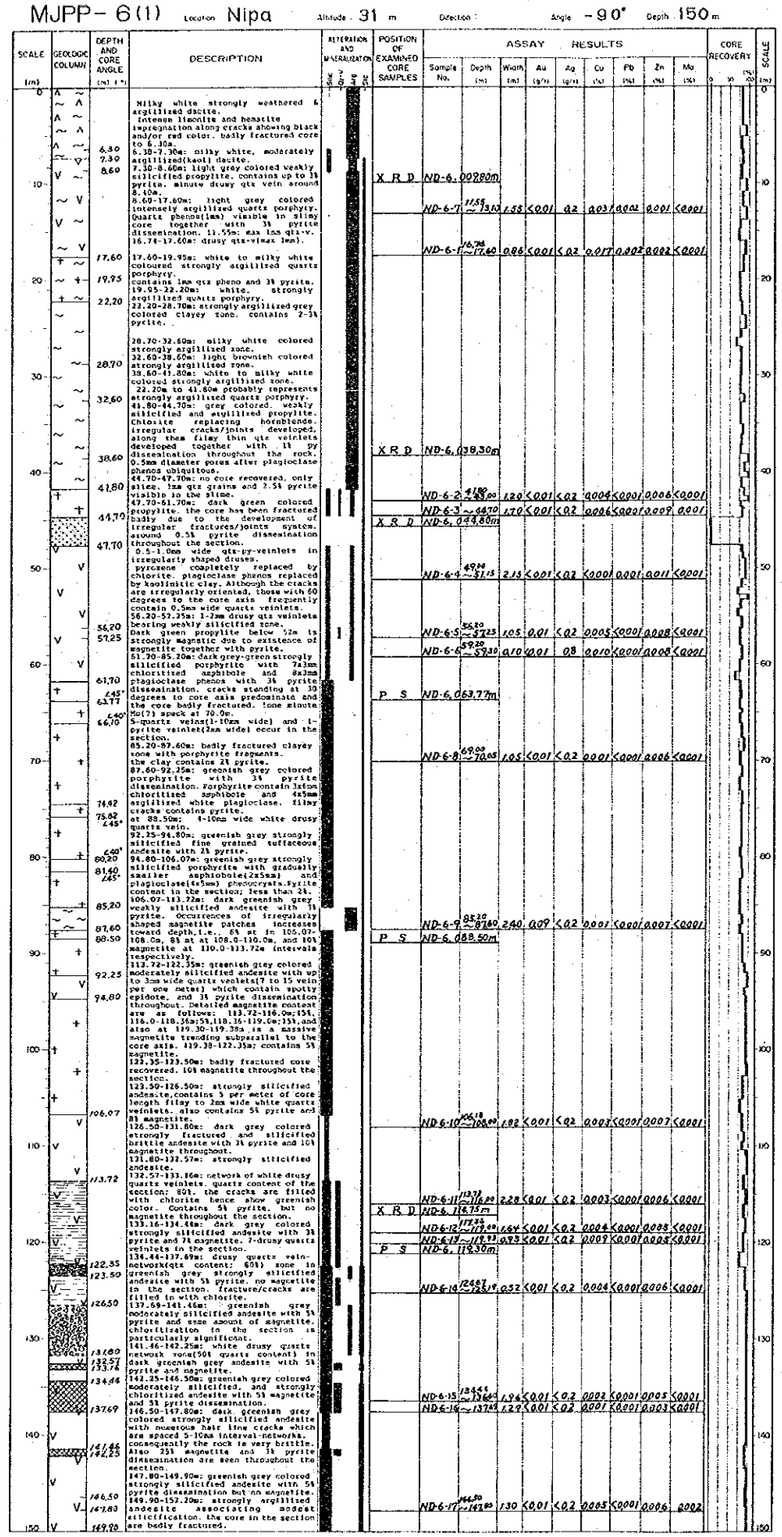

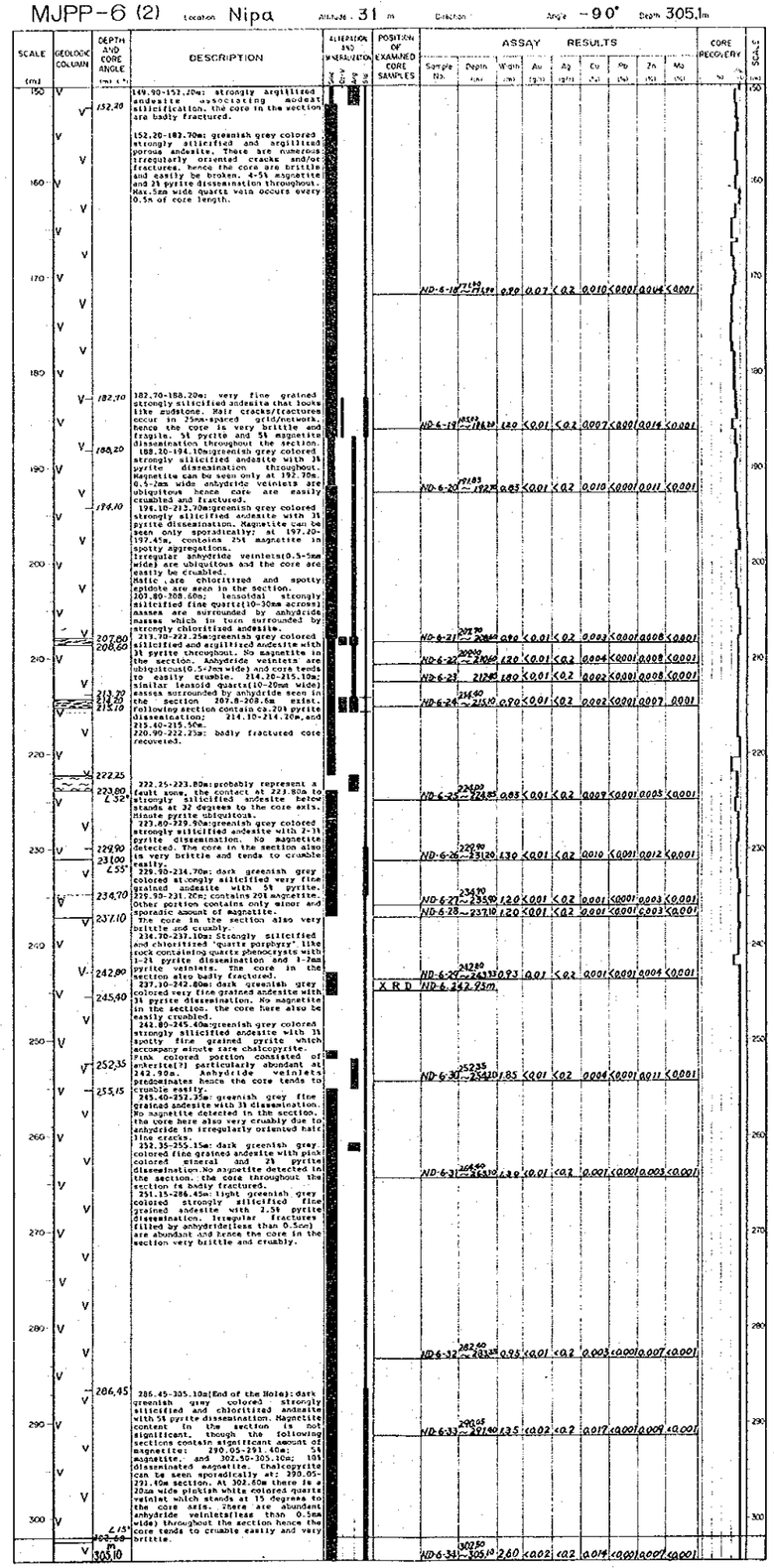

Figure 21 Geologic Log of MJPP–6, Nipa, 1992

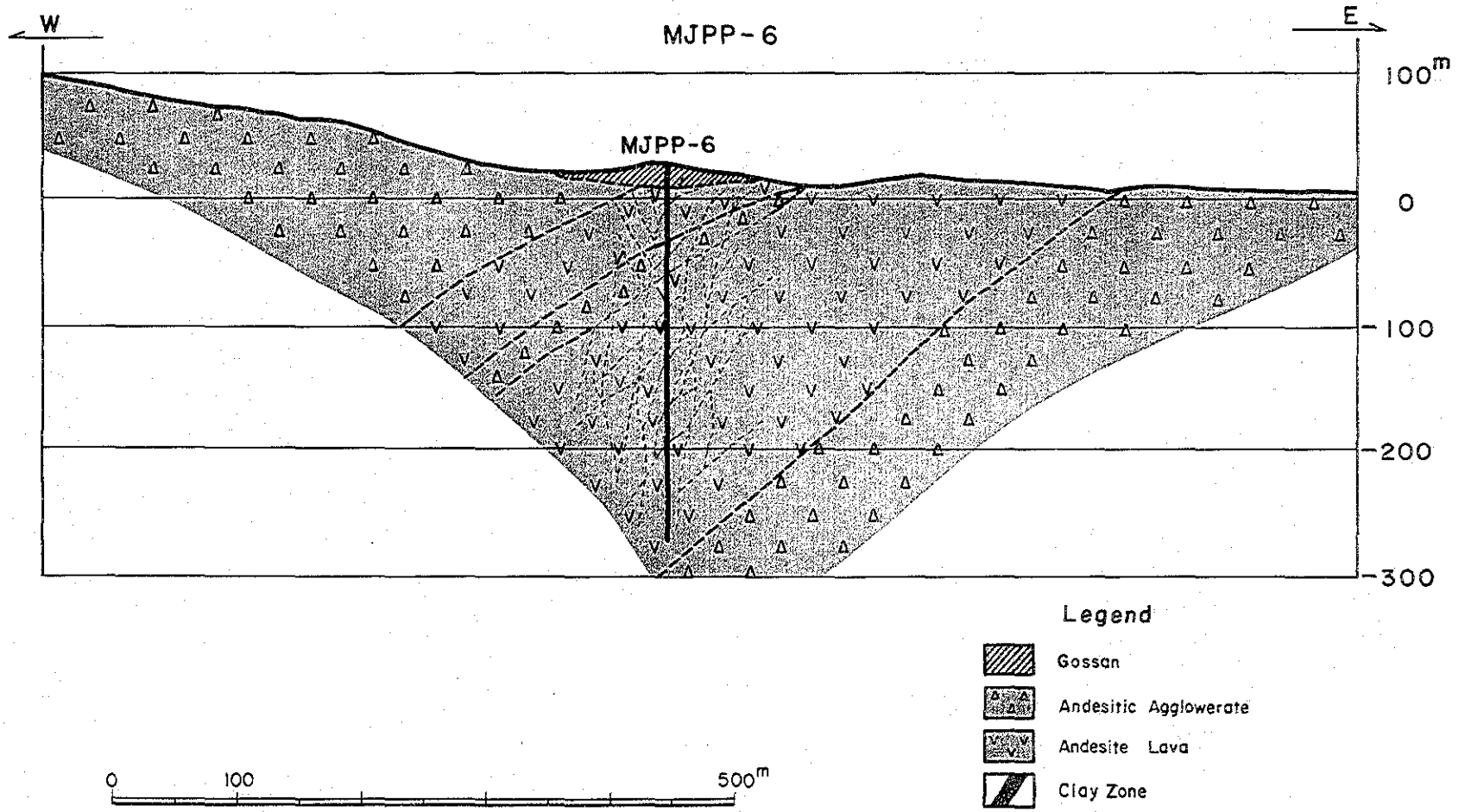

Figure 22 Geologic Cross Section Through Drill Hole, Nipa

In the Puntales sub-target area, a hole was drilled to explore the gossanous zone and the surrounding geochemical anomaly at depth. The drill hole intersected silicification and argillization only with feeble mineralization of Cu and Mo. The gossanous zones were presumably formed by deep weathering and leaching through intensely fractured and altered zones.

The geochemical prospecting in the Puntales sub-target area found an anomalous zone in Mo to the west of the drill hole location. However, there may be a very small possibility for the Mo anomaly to extend to a considerable area, judging from the results of the semi-detailed geochemical prospecting. Cu geochemical anomalies were also located to the southwest and the west of the drill hole location but were discontinuous and low in Cu values. The Puntales sub-target area does not warrant further exploration with these results of the current project.

The Apiton sub-target area was prospected by a detailed soil geochemical survey to study gold anomalies defined by the semi-detailed soil geochemical prospecting in the entire Nipa target area. The detailed soil geochemical prospecting in the Apiton sub-target area indicated a relatively high average Au value of 19 ppb, and outlined Au anomalies by therehold values of Au 37 ppb (M+2SD) on ridges to the south and the southwest of Mt. Apiton. These anomalies coincide with gold anomalies outlined by the semi-detailed geochemical prospecting. The gold anomalies located specifically on ridges such as these, may suggest a possibility of gold concentrations and alterations of a similar type to that in the Mt. Upao and the Madarag target areas. However, there may be little possibility that the gold mineralization of this type has been up-graded to ore grades, judging from the assay results of the drill core samples in both target areas.

2–5 Binanan

2–5–1 Geology Alteration, and Mineralization

(1) Geology

The Sibala formation, consisting mainly of andesitic volcanics subjected to green alteration, is distributed in this target area as in the other target areas. The Sibala formation in this target area, unlike other target areas, mainly comprises pyroclastics such as agglomerates which are interbedded with an alternation of sandstone, mudstone and tuff in the southwestern part of Binanan Island. The alternation strikes in the NNW–SSE direction and dips 30° to 40° to the southwest. Small dikes of quartz porphyry intrude the Sibala formation in the southeastern part of the island. The altered andesite member characterized by hematitization is distributed on ridges also in this target area as in the other target areas.

(2) Alteration

The Sibala formation is green coloured due essentially to propylitic alteration forming quartz and chlorite, except for the altered andesite member on the ridges, in which quartz, kaolinite and hematite are common alteration minerals.

(3) Mineralization

No records of exploration are known in this target area, though Au, As, Hg, Te, Se and Tl geochemical anomalies have been located (MMAJ/JICA–MGB, 1989).

2–5–2 Geochemical Prospecting

(1) Methodology

Detailed soil geochemical sampling on a grid basis (line spacing; 200 meters, sampling interval; 50 meters, number of samples; 100) was carried out for the Binanan target area and semi–detailed sampling on a ridge–and–spur basis (number of samples; 40) for the periphery of the target area. Chemical analysis of the soil samples was made for eleven elements, Au, Ag, As, Bi, Cu, Hg, Mo, Pb, Sb, Zn and Mn.

(2) Data Processing and Statistical Analysis

Statistical parameters are shown in Table 25 for the univariate analysis and in Table 26 for the principal component analysis. Distributions of geochemical anomalies are illustrated in Figure 23.

Au values were higher than the lower detection limit in 97 % of the total samples, with a maximum of 116 ppb and an average of 8.9 ppb and were generally higher than those in other target areas. As values were very high in this target area, with a maximum of 807 ppm and an average of 26.9 ppm. Averages of Cu, Pb and Zn values were nearly equal to or slightly lower than those in the neighbouring Nipa area, though their maximum values in this area were lower.

The principal component analysis was made for eight elements excluding Bi and Hg, most values of which were lower than the detection limits. The first principal component accounts for 43.4 % of the total variance with positive contributions in Mn, Zn and Cu and negative contributions in Mo, Bi, Pb, As and Au. Mn and Zn contribute to this component in the opposite sense to Au, As and Mo as is the case in other target areas. However, the Mo factor loading for the first principal

Table 2 5 Statistic Parameters for Soil Samples, Binanan, 1991

Statistic Parameters

COMP. NAME	UNIT	NUM. DATA	MAXIMUM	MINIMUM	MEAN (M)	STD. DEV. (SD)	M-2*SD	M-SD	M+SD	M+2*SD
AU	ppb	136	116	1	8.9	0.479	1.0	3.0	26.8	80.7
AG	ppm	57	0.30	0.05	0.067	0.183	0.028	0.043	0.103	0.159
AS	ppm	140	807.0	2.6	26.82	0.521	2.44	8.11	89.36	296.61
BI	ppm	86	7.2	0.2	0.34	0.333	0.07	0.16	0.74	1.59
CU	ppm	140	99.8	2.8	19.47	0.365	3.63	8.41	45.08	104.36
HG	ppm	34	0.7	0.1	0.14	0.208	0.05	0.08	0.22	0.36
MO	ppm	140	16.8	0.2	1.13	0.412	0.17	0.44	2.92	7.55
PB	ppm	140	44.5	1.5	5.52	0.264	1.64	3.01	10.14	18.63
SB	ppm	59	10.6	0.2	0.64	0.448	0.08	0.23	1.79	5.02
ZN	ppm	140	101	1	23.2	0.460	2.8	8.0	66.8	192.7
MN	ppm	140	2506	22	439.8	0.472	50.1	148.4	1303.2	3862.1

Correlation Matrix

	AU	AG	AS	BI	CU	HG	MO	PB	SB	ZN	MN
AU	---	57	136	82	136	32	136	136	59	136	136
AG	0.366	---	57	35	57	15	57	57	29	57	57
AS	0.658	0.316	---	86	140	34	140	140	59	140	140
BI	0.032	0.193	0.156	---	86	21	86	86	40	86	86
CU	0.014	0.074	0.048	-0.066	---	34	140	140	59	140	140
HG	0.077	0.338	0.337	0.368	-0.089	---	34	34	19	34	34
MO	0.525	0.169	0.537	0.438	-0.137	0.125	---	140	59	140	140
PB	0.442	0.199	0.404	0.287	-0.161	-0.043	0.456	---	59	140	140
SB	0.227	0.400	0.612	0.592	-0.031	0.663	0.425	0.230	---	59	59
ZN	-0.187	-0.129	-0.224	-0.550	0.558	-0.114	-0.594	-0.241	-0.361	---	140
MN	-0.173	-0.143	-0.088	-0.543	0.397	-0.104	-0.586	-0.181	-0.325	0.765	---

Table 26 Results of Principal Component Analysis for Soil Samples, Binanan 1991

PRIN COMP	EIGEN VALUE	CONTRIB	CUM CONTRIB		AU	AS	BI	CU	MO	PB	ZN	MN
P 1	3.471	0.434	0.434	EIGENVECTOR	-.298	-.301	-.333	.211	-.459	-.312	.438	.408
				FACTOR LOADING	-.556	-.561	-.620	.394	-.855	-.581	.816	.757
				CONTRIBUTION	.309	.315	.385	.155	.731	.338	.666	.572
P 2	1.782	0.223	0.657	EIGENVECTOR	.495	.491	-.216	.390	.129	.268	.328	.346
				FACTOR LOADING	.660	.656	-.288	.520	.172	.358	.438	.461
				CONTRIBUTION	.436	.430	.083	.270	.029	.128	.192	.213
P 3	0.947	0.118	0.775	EIGENVECTOR	-.203	-.045	.615	.728	.123	-.130	.078	-.102
				FACTOR LOADING	-.197	-.044	.599	.708	.119	-.126	.076	-.100
				CONTRIBUTION	.039	.002	.358	.502	.014	.016	.006	.010
P 4	0.699	0.087	0.862	EIGENVECTOR	-.240	-.207	.286	-.126	-.184	.830	.152	.237
				FACTOR LOADING	-.200	-.173	.239	-.105	-.154	.694	.127	.198
				CONTRIBUTION	.040	.030	.057	.011	.024	.481	.016	.039
P 5	0.429	0.054	0.916	EIGENVECTOR	.276	-.650	-.350	.252	.269	.221	.169	-.406
				FACTOR LOADING	.181	-.428	-.230	.165	.176	.145	.111	-.266
				CONTRIBUTION	.033	.181	.053	.027	.031	.021	.012	.071
P 6	0.307	0.038	0.954	EIGENVECTOR	-.648	.158	-.364	.067	.627	.097	-.026	.118
				FACTOR LOADING	-.360	.088	-.202	.037	.347	.054	-.014	.065
				CONTRIBUTION	.129	.008	.041	.001	.121	.003	.000	.004
P 7	0.199	0.025	0.979	EIGENVECTOR	.260	-.395	.277	-.215	.470	-.220	-.020	.620
				FACTOR LOADING	.116	-.176	.123	-.096	.209	-.098	-.009	.276
				CONTRIBUTION	.013	.031	.015	.009	.044	.010	.000	.076
P 8	0.167	0.021	1.000	EIGENVECTOR	-.047	.140	.225	-.379	.197	-.133	.801	-.294
				FACTOR LOADING	-.019	.057	.092	-.155	.080	-.055	.327	-.120
				CONTRIBUTION	.000	.003	.008	.024	.006	.003	.107	.014

component reaches 70 % in this target area, being characteristically higher than other areas. Negative scores of this component are considered to indicate Mo concentration rather than Au concentration, judging from the higher contribution of Mo than Au. However, the Mo values of this area are generally lower than those of the Nipa and Madarag areas and the first principal component is not considered to be indicative of molybdenum mineralization. The second principal component accounts for 22.3 % of the total variance with significant contributions of Au, As, Cu and Pb. This component indicates Au concentration accompanied by As, Cu and Pb. The third principal component accounts for 11.8 % of the total variance with contributions largely of Cu and Bi. Though this component may indicate copper concentration accompanied by bismuth, generally low copper values with a maximum of 99.8 ppm imply that there is a very small possibility of copper mineralization of any commercial significance. The cumulative variance to the third principal component accounts for 77.5 % of the total variance.

2–5–3 Assessment of Results

The geochemical Au, As, Hg, Te, Se and Tl anomalies which had been outlined by the past investigations were subjected to detailed and semi–detailed geochemical prospecting in the current project.

The current results indicated higher Au and As concentrations than in the other three target areas. Geochemical anomalies which were outlined by a gold threshold value or by scores of the second and third principal components are sporadically distributed in this target area. A first principal component anomaly was also outlined in the northeastern part of Binanan Island.

However, the Au geochemical anomalies in the univariate analysis, and the anomalies of the second principal component with high Au and As factor loadings and of the third principal component with a high Cu factor loading are sporadically distributed, which implies that there is little potential for ore deposits of commercial importance in this target area.

The anomaly of the first principal component, which has a high Mo factor loading, was outlined in the northeastern part of Binanan Island. However, the Mo values of this area are generally low in comparison with those in Nipa and Madarag target areas. Accordingly, it is considered that there is little possibility for intense molybdenum mineralization below this anomaly.

The Binanan area was excluded from the drilling target in the 1992 compaign for the reason, in addition to the above, that the area on an isolated small island is limited in space for exploitation even though potentials for concentrations of useful metallic minerals may be assumed.

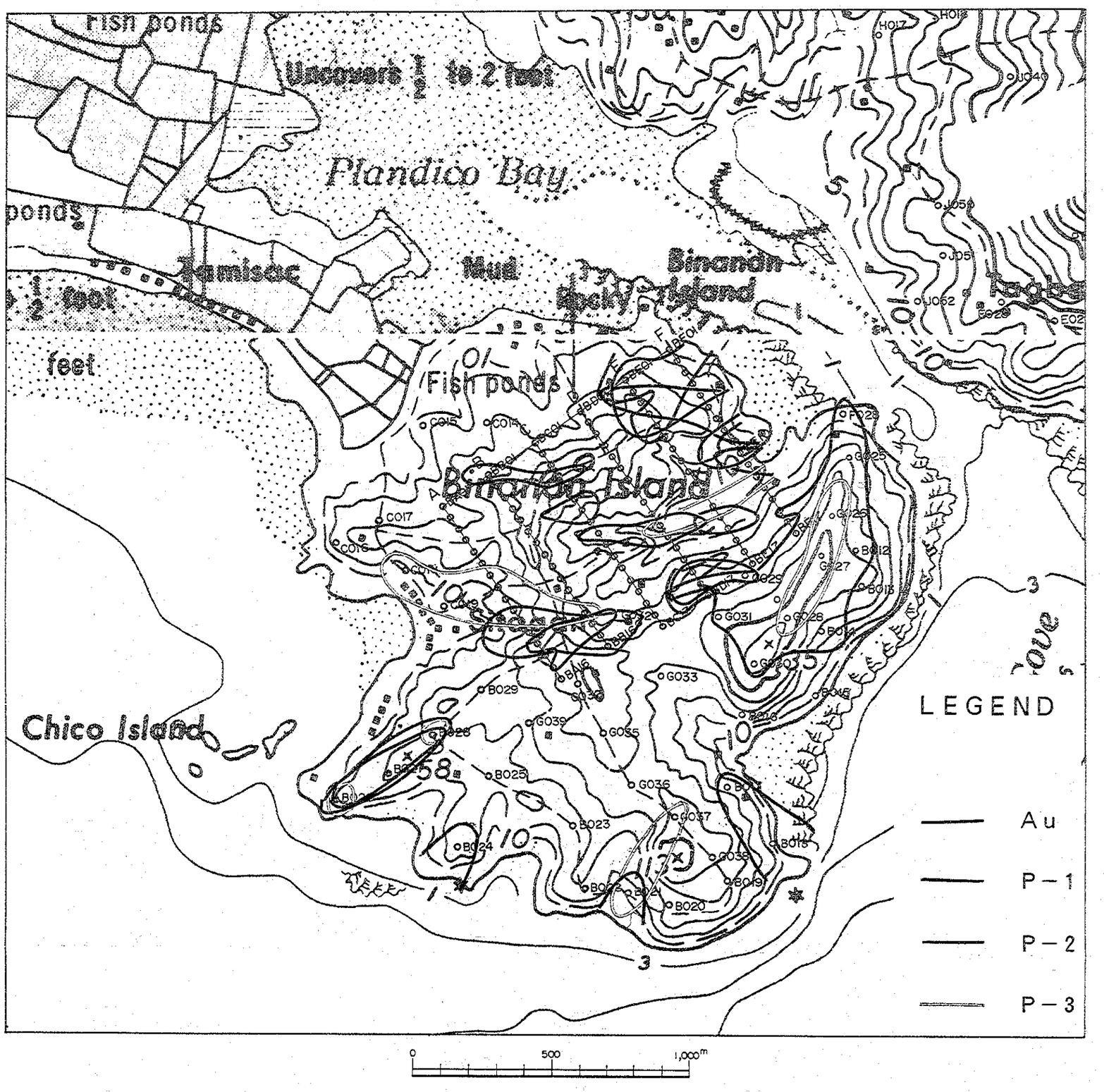

Figure 23 Geochemical Anomaly Map, Binanan, 1991

Chapter 3 Conclusions and Recommendations

3–1 Conclusions

Cooperative Mineral Exploration Project was carried out for two years, 1991 and 1992, in Panay Region of the Republic of Philippines by cooperation between MMAJ/JICA (Japan Side) and MGB (Philippines Side). The project was to explore mineral resources in four target areas, Mt. Upao, Madarag, Nipa and Binanan, in Panay Region by geological mapping, detailed and semi–detailed geochemical prospecting, trenching and drilling.

The results of those work are summarized as follows;

(1) The Sibala formation, consisting mainly of Tertiary volcanics, is widely distributed in the project area with intrusions of holocrystalline granitoids, quartz porphyries and andesite. The Guimaras Belt running in the NNE–SSW direction in western Panay, is characterized by holocrystalline intrusions, while the Negros Belt, running in the same direction in the eastern edge of the region, comprises the Botlog and Pan de Azucar volcanics of Quaternary age.

(2) Intensely hematitic volcanics which had previously been distinguished as the Odiongan volcanics were proved to belong to the Sibala formation as the results of drilling which indicated no hiatus or stratigraphic discontinuity between the volcanics and the underlying volcanic rocks of the Sibala formation. The hematitic volcanics have been subjected to intense pyritization, argillization and silicification and show characteristic features due to surficial oxidation and leaching.

(3) The volcanic rocks of the Sibala formation have been generally subjected to propylitic alteration, commonly characterized by such neutral alteration mineral assemblages as quartz ± chlorite ± sericite ± sericite/montmorillonite interstratified minerals. The hematitic altered volcanic rocks, the former Odiongan volcanics, are commonly developed with such acidic alteration minerals as quartz, kaolinite and alunite often accompanied by dickite, pyrophyllite and diaspore which indicate a high temperature acidic alteration facies. These high temperature acidic alteration minerals are usually formed along faults and fractured zones, which suggests high temperature hydrothermal activities along such faults and fracture zones at various stages in the past. Dickite, pyrophyllite and diaspore are very common alteration minerals in the Madarag target area.

(4) A number of geochemical anomalies in Au, As, Sb and base metal elements were outlined in the Mt. Upao, Madarag, Nipa and Binanan target areas as the results of the geochemical prospecting. Particularly in the Mt. Upao target area, a gold anomaly, outstandingly higher than the background, was outlined with a general trend in the N–S direction. To verify these geochemical anomalies, trenching and drilling were carried out for the Mt. Upao and Madarag target areas, and drilling and additional detailed geochemical prospecting for the Nipa target area, in the 1992 field campaign.

Assessments of mineral potential for each target area are summarized, on the basis of the results of these works, as follows;

Mt. Upao

The trenching confirmed zones of gold concentration which had been outlined by soil geochemistry. However, the three holes which were drilled below the gold concentration zone on the surface indicated disappointing results which failed to prove any gold mineralization of commercial significance although gold concentration due to hydrothermal activities were intersected in parts. Based

on the results of the principal component analysis, the surficial gold concentration is considered to have formed by secondary enrichment of gold in the hydrothermally altered zone due to weathering and leaching. Accordingly, it is concluded that this target area is low in potential for commercial mineral resources.

Madarag

Gold concentrations were identified by trenching over a geochemical gold anomaly and were drilled by two holes with an inclination of −40 degree. The drill holes intersected extensive copper mineralization due to hydrothermal activities, though grades failed to reach a commercial degree. The mineralization consisted mainly of chalcopyrite, pyrite and magnetite accompanied by minor arsenic copper minerals in parts. This type of mineralization may be of academic interest and has very little chance of forming a sizable body with a commercial grade. Accordingly it is concluded that this target area is low in potential for commercial mineral resources. The geochemical gold anomalies are considered to have been formed by surficial secondary enrichment due to weathering and leaching in the hydrothermally altered zones carrying copper minerals.

Nipa

A vertical hole which was drilled to explore gossanous zones with geochemical Mo and Cu anomalies to the north of Puntales village, intersected at depth highly fractured zones with intense hydrothermal alteration but failed to locate any Cu–Mo mineralization. A base metal ore deposit consisting of quartz veins with some gold values, located to the south of Nipa village was not associated with geochemical anomalies which would support spacial extensions of its mineralization. In addition, the quartz veins are extremely variable in their width and tend to be discontinuous. The ore deposit is very low in its grades of base and precious minerals and is too closely located to the coast for an extensive exploitation. The additional detailed geochemical prospecting verified the nature of the gold geochemical anomalies on the top of ridges near Mt. Apiton in the southern part of this target area, and indicated that similar gold enrichment as in Mt. Upao or Madarag may be expected. Judging from drilling results in these area, the mineralization is not considered to form ore deposits of any commercial significance.

With all the above mentioned results, the Nipa target area is also concluded to be of very little interest for commercial mineralization.

Binanan

The gold and arsenic geochemical values of this target area were apparently higher than those of the other three target areas. An anomaly of the first principal component in which the Mo factor loading was outstanding, was outlined in the northeastern part of the area. However, the Mo values of this area were generally lower than those in Madarag or Nipa. Geochemical gold anomalies and anomalies in the second and third principal components characterized by high factor loadings of Au, As and Cu respectively were sporadically distributed. Accordingly, it is concluded that the anomalies described above have very little possibility to form any commercially significant mineralization. In addition, this target area is located on an isolated island with the highest elevation of 70 meters above sea level, and is spacially limited for an extensive exploration of mineral resources, even if any concentration of useful metallic elements existed.

3-2 Recommendation

The eastern Panay region was systematically explored in this project through a series of stages beginning with the reconnaissance stream sediment sampling, followed-up by the regional, semi-detailed and detailed soil geochemical prospecting and ending with the trenching and drilling.

The project located hydrothermal alteration zones associated with gold, copper, molybdenum and/or other metallic mineralization in the four target areas, Mt. Upao, Madarag, Nipa and Binanan, in eastern Panay. These zones were well defined as geochemical anomalies.

The holes which were drilled in these zones, however, failed to discover mineralization with any commercial significance. Accordingly, it is concluded that the Panay region warrants no further exploration of advanced stages.

Lmited exploration work may be recommended for a part of the Madarag target area where an extensive high temperature alteration zone has been located in association with relatively high copper and gold concentrations. This zone is worthwhile to be verified for a possibility of commercial exploration, although there is very little possibility for the zone to form a large mineralized body.

REFERENCES

Abiog, D.B.(1970); Report on the Geological Inspection of Copper–Gold and Iron Deposits in Concepcion and Nueva Valencia, Guimaras sub–Province, Iloilo., Bureau of Mines and Geoscience, unpublished report.

Bureau of Mines and Geoscience(1981); Geology and Mineral Resources of the Philippines, Vol.1, Geology.

Bureau of Mines and Geoscience(1986); Geology and Mineral Resources of the Philippines, Vol.2, Mineral Resources.

Capistrano, P.M.(1953); Geology and Copper Deposits of Pilar Area and Vicinity., Bureau of Mines and Geoscience, unpublished report.

Estanpigas, P.S.(1968); Geologic Investigation of Pilar Copper Mines, Pilar, Capiz, Panay Island.

Francisco, F.U.(1949); Report on the Pyrite Possibilities of the Pilar Copper District, Pilar, Capiz.

Hashimoto, W.(1981); Contribution to the Geology and Paleontology of Southeast Asia., ccx VII, Geologic Department of Philippines.

Hashimoto, W.(1982); Paleontology of the Philippines Supplement 1 (1969–1981).

MMAJ & JICA (1986); The Mineral Exploration – Mineral Deposits and Tectonics of Two Contrasting Geologic Environments in the Republic of Philippines, Geology and Geochemistry in Eastern Panay Island (in Japanese).

MMAJ & JICA (1987); The Mineral Exploration – Mineral Deposits and Tectonics of Two Contrasting Geologic Environments in the Republic of Philippines, Phase II Geology and Geochemistry in Cebu Island, Panay Island and Romblon Island.

MMAJ & JICA (1989); The Mineral Exploration – Mineral Deposits and Tectonics of Two Contrasting Geologic Environments in the Republic of Philippines, Geology and Geochemistry in Panay–Sara Area.

MMAJ & JICA (1992); The Cooperative Mineral Exploration, Geological and Geochemical Survey in Panay Area, Phase II.

MMAJ & JICA (1993); The Cooperative Mineral Exploration, Geological and Geochemical Survey in Panay Area, Phase III.

GEOLOGICAL MAP OF THE PANAY AREA BY MMAJ/JICA-MGB

SUMMARISING THE RESULTS OF MINERAL EXPLORATION 1991-1992

Scale 1 : 50,000

REPORT ON THE MINERAL EXPLORATION
IN THE PANAY AREA
REPUBLIC OF THE PHILIPPINES

PREPARED BY JAPAN INTERNATIONAL COOPERATION AGENCY (JICA) AND
METAL MINING AGENCY OF JAPAN (MMAJ) IN COOPERATION WITH THE MINES
AND GEOSCIENCES BUREAU OF THE REPUBLIC OF THE PHILIPPINES (MGB)
FEBRUARY, 1993

LOCATION MAP OF THE PANAY AREA

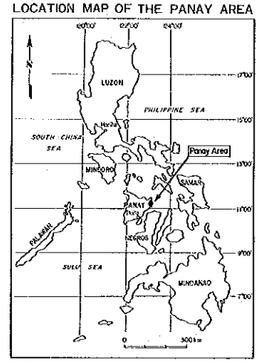

INDEX MAP OF THE SURVEY AREAS

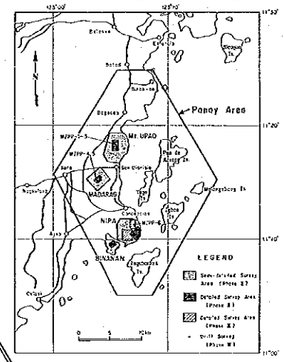

REGIONAL GEOLOGY IS COMPILED FROM THE MINERAL EXPLORATION PROJECT IN 1988 CARRIED OUT BY MMAJ/JICA-MGB

Mt. UPAO AREA

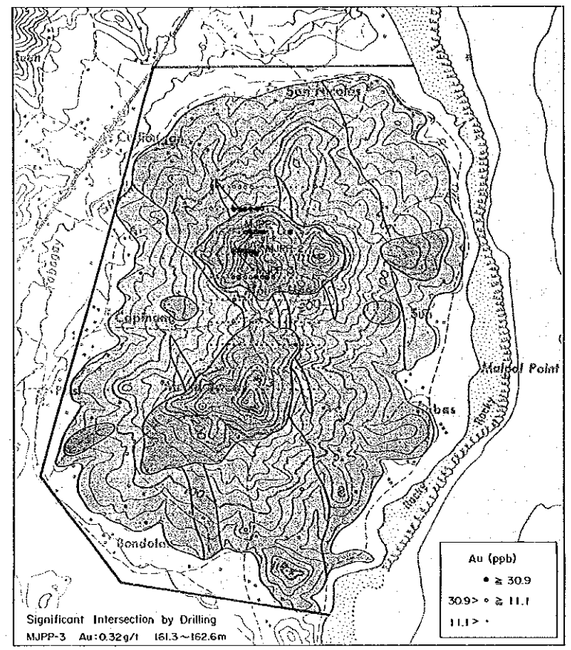

MADARAG AREA

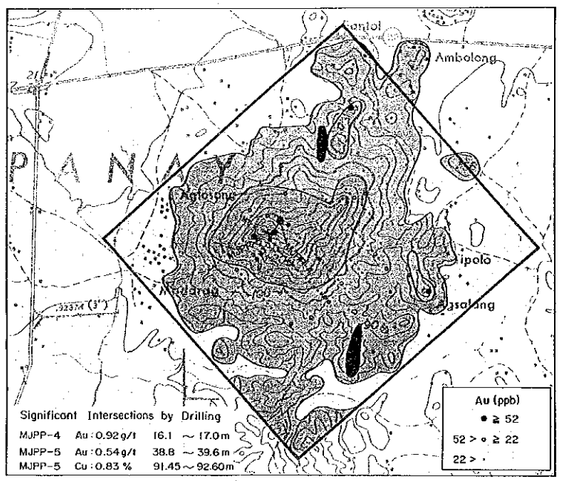

NIPA, BINANAN AREAS